Competition Reaction Based Prediction of Polyamines' Stepwise Protonation Constants: a Case Study Involving 1,4,7,10-tetrazadecane (2,2,2-tet)

Adeyinka Adedapo, Bryan William Bulling and Ignacy Cukrowski*.

Department of Chemistry, Faculty of Natural and Agricultural Sciences, University of Pretoria, Lynnwood Road, Hatfield, Pretoria 0002

*Corresponding author: ignacy.cukrowski@up.ac.za

Supplementary Information

PART 1

Comments on conformational search procedure and competition reactions considered.

For both 3,2,3-tet and 2,2,2-tet, when the implicit solvation model was to be implemented, we varied each rotatable bond in steps of 60^0 each and retained thirty lowest energy LECs. These were fully optimized using the implicit solvation model to describe solvent environment in order to locate representative set of LECs. In implementing the discrete continuum solvation model for 2,2,2-tet, we used a similar conformational search protocol to that which was implemented in the case of implicit solvation but only retained twenty LECs based on their relative MMFF(aq) energies because our previous conformational analysis of 2,2,2-tet indicated that its representative LECs would most likely be found among the ten LECs obtained from an MMFF(aq) based search of its conformational space.[1] However, since 3,2,3-tet has a greater number of rotatable bonds than 2,2,2-tet due to its longer alkyl chain length and there has been no conformational analysis work reported for it, we carried out the conformational search for its LECs in the presence of explicit solvent molecules in two stages. This was to enable us investigate which torsional angle increment (60° or 120°) is best for locating its low energy conformers:

- In the first stage, each rotatable bond was allowed to change in 60^0 steps and thirty unique lowest energy conformers were retained based on their relative MMFF(aq) energies.
- For the second stage rotation of bonds was allowed in 120^0 steps and thirty unique lowest energy conformers were also retained based on their relative MMFF(aq) energies.

Conformers obtained from both stages were combined and for each tautomer examined, only the thirty unique LECs out of sixty generated, were selected for further optimizations. After full optimization, a thorough examination and analysis of the final structures and energies of LECs generated for 3,2,3-tet showed that in general most of its lowest in energy conformers were from the MM-based conformational search when each rotatable bond was allowed to vary in steps of 120°. Hence, as pointed out in our previous work on 2,2,2-tet, to identify representative LECs of any given aliphatic polyamine, it is sufficient to vary its rotatable bonds in increments of 120° each.

As depicted in Scheme 1 in the main body of the text, which involves all possible protonation sites of 2,2,2-tet (here $L^{(1)}$) and 3,2,3-tet (here $L^{(2)}$) when they are singly protonated, one must consider a number of possible reactions which indeed might take place in a real competition

experiment in a solution. To reflect this fact, a general form of competition reaction 1 can be expressed in the following forms

$$L^{(1)} + HL_p^{(2)} = HL_p^{(1)} + L^{(2)} \qquad \Delta G^{(1)}_{HL_p^{(1)},HL_p^{(2)}} \qquad \text{(S1)}$$

$$L^{(1)} + HL_p^{(2)} = HL_s^{(1)} + L^{(2)} \qquad \Delta G^{(1)}_{HL_s^{(1)},HL_p^{(2)}} \qquad \text{(S2)}$$

$$L^{(1)} + HL_s^{(2)} = HL_p^{(1)} + L^{(2)} \qquad \Delta G^{(1)}_{HL_p^{(1)},HL_s^{(2)}} \qquad \text{(S3)}$$

$$L^{(1)} + HL_s^{(2)} = HL_s^{(1)} + L^{(2)} \qquad \Delta G^{(1)}_{HL_s^{(1)},HL_s^{(2)}} \qquad \text{(S4)}$$

$$L^{(1)} + HL_p^{(2)} + HL_s^{(2)} = HL_p^{(1)} + L^{(2)} \qquad \Delta G^{(1)}_{HL_p^{(1)},HL_{p+s}^{(2)}} \qquad \text{(S5)}$$

$$L^{(1)} + HL_p^{(2)} + HL_s^{(2)} = HL_s^{(1)} + L^{(2)} \qquad \Delta G^{(1)}_{HL_s^{(1)},HL_{p+s}^{(2)}} \qquad \text{(S6)}$$

$$L^{(1)} + HL_p^{(2)} = HL_p^{(1)} + HL_s^{(1)} + L^{(2)} \qquad \Delta G^{(1)}_{HL_{p+s}^{(1)},HL_p^{(2)}} \qquad \text{(S7)}$$

$$L^{(1)} + HL_s^{(2)} = HL_p^{(1)} + HL_s^{(1)} + L^{(2)} \qquad \Delta G^{(1)}_{HL_{p+s}^{(1)},HL_s^{(2)}} \qquad \text{(S8)}$$

$$L^{(1)} + HL_p^{(2)} + HL_s^{(2)} = HL_p^{(1)} + HL_s^{(1)} + L^{(2)} \qquad \Delta G^{(1)}_{HL_{p+s}^{(1)},HL_{p+s}^{(2)}} \qquad \text{(S9)}$$

where subscripts ‘s’ and ‘p’ denote a primary and secondary N-atom of a ligand being protonated and the sequence of subscripts in the $\Delta G^{(1)}_{CRn}$ expressions shows tautomers of $HL^{(1)}$ and $HL^{(2)}$ involved; their sequence follows the way $\Delta G^{(1)}_{CRn}$ is calculated ($G_{products} - G_{reactants}$) and, *e.g.*, for $\Delta G^{(1)}_{CRn} = \Delta G^{(1)}_{HL_{p+s}^{(1)},HL_p^{(2)}}$ (expression S7) it means that two tautomers of a singly protonated polyamine under investigation, $HL_p^{(1)}$ and $HL_s^{(1)}$, and by default the free reference ligand $L^{(2)}$ were formed as a result of reaction between $L^{(1)}$ (by default) and the tautomer of the singly protonated reference polyamine with the primary N-atom being protonated, hence $HL_p^{(2)}$.

1. Adeyinka, A.S.; Cukrowski, I.; *J. Mol Model.* **2015**, 21, 162.

PART 2

Input structures used for the conformational search

(a)

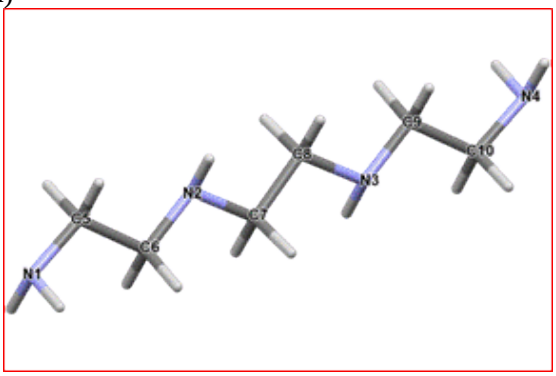

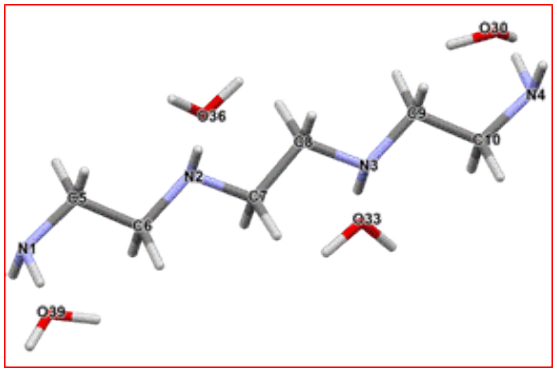

(b)

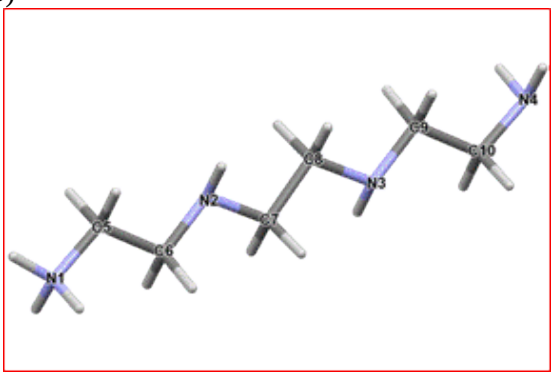

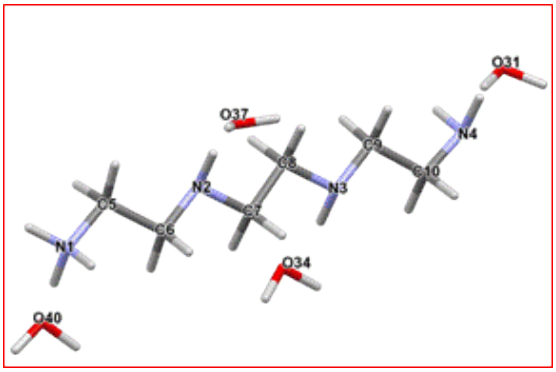

(c)

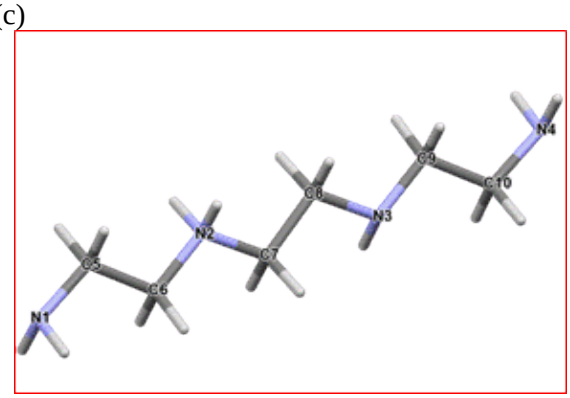

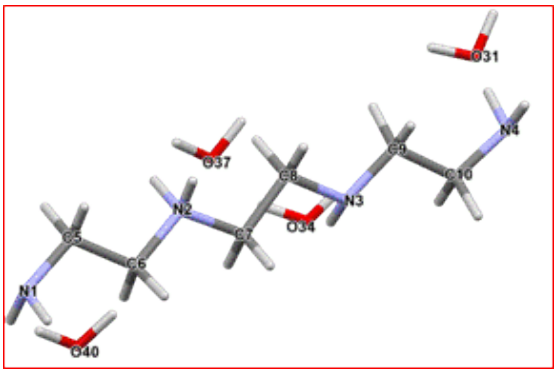

(d)

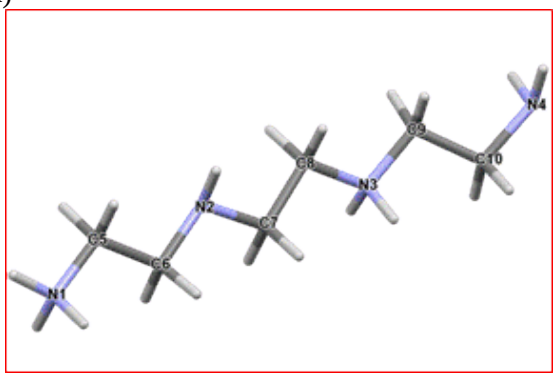

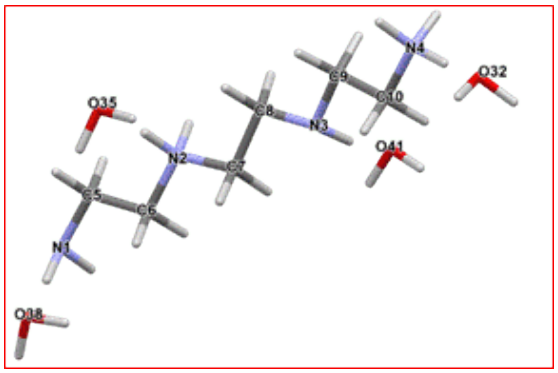

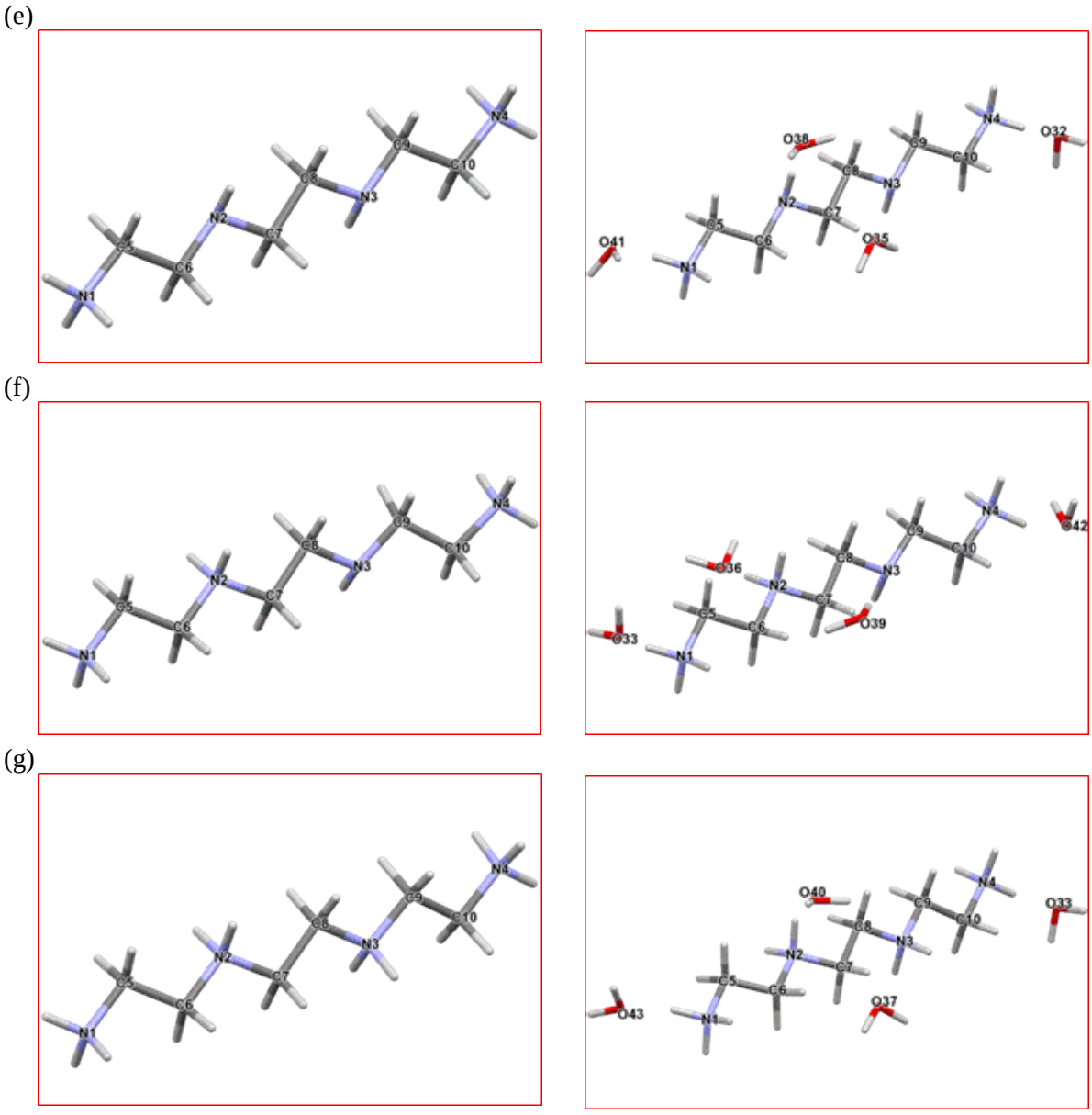

Figure S1. Capped-stick representation of linear structures of H_nL^{n+} forms of 2,2,2-tet with and without explicit water molecules used as inputs for conformational search by MM, also showing atoms' numbering: part (a) – L; part (b) – HL_{N1} (HL_p); part (c) – HL_{N2} (HL_s); part (d) – H_2L_{N1N3} (H_2L_{ps}), part (e) – H_2L_{N1N4} (H_2L_{pp}); part (f) – H_3L_{N1N2N4} (H_3L_{psp}) and part (g) – H_4L.

(a)

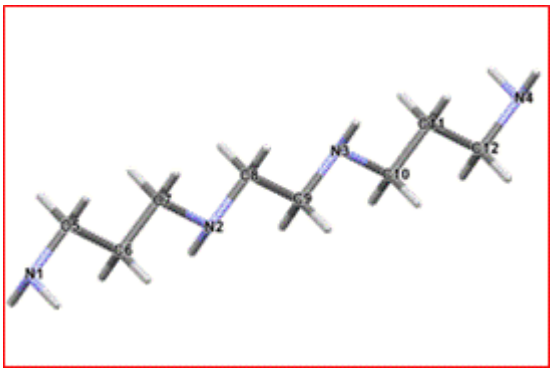
N4
C11
C12
N3
C10
C9
N2
C8
C7
C6
C5
N1

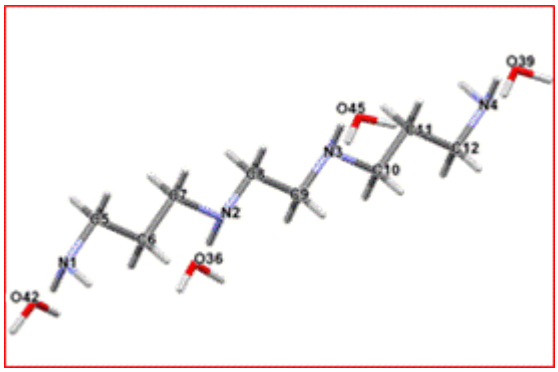
O39
O45
N4
C11
C12
N3
C10
C9
N2
C7
C6
C5
N1
O36
O42

(b)

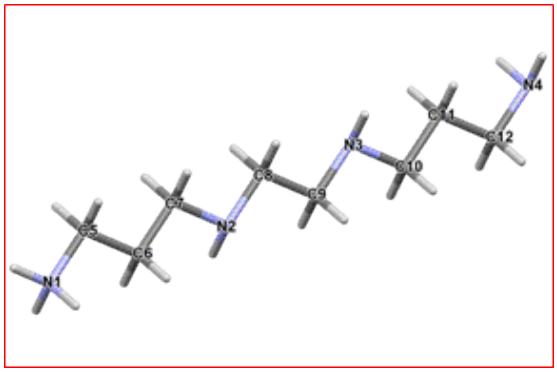
N4
C11
C12
N3
C10
C9
N2
C8
C7
C6
C5
N1

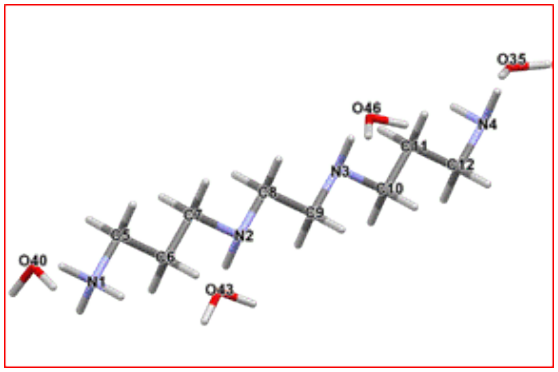
O35
O46
N4
C11
C12
N3
C10
C9
N2
C8
C7
C6
C5
N1
O40
O43

(c)

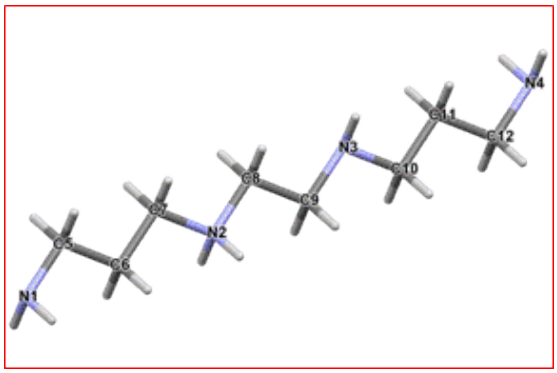
N4
C11
C12
N3
C10
C9
N2
C8
C7
C6
C5
N1

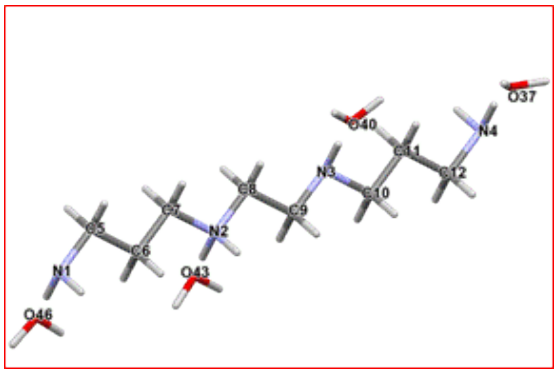
O37
O40
N4
C11
C12
N3
C10
C9
N2
C8
C7
C6
C5
N1
O43
O46

(d)

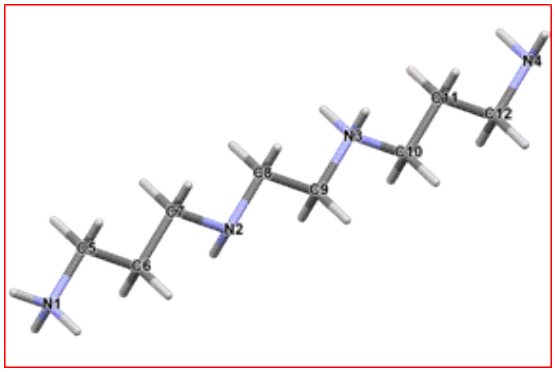
N4
C11
C12
N3
C10
C9
N2
C8
C7
C6
C5
N1

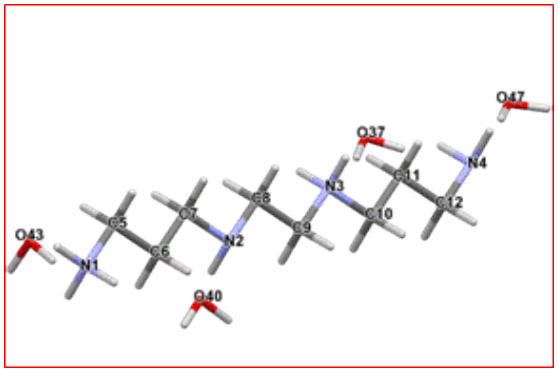
O47
O37
N4
C11
C12
N3
C10
C9
N2
C8
C7
C6
C5
N1
O43
O40

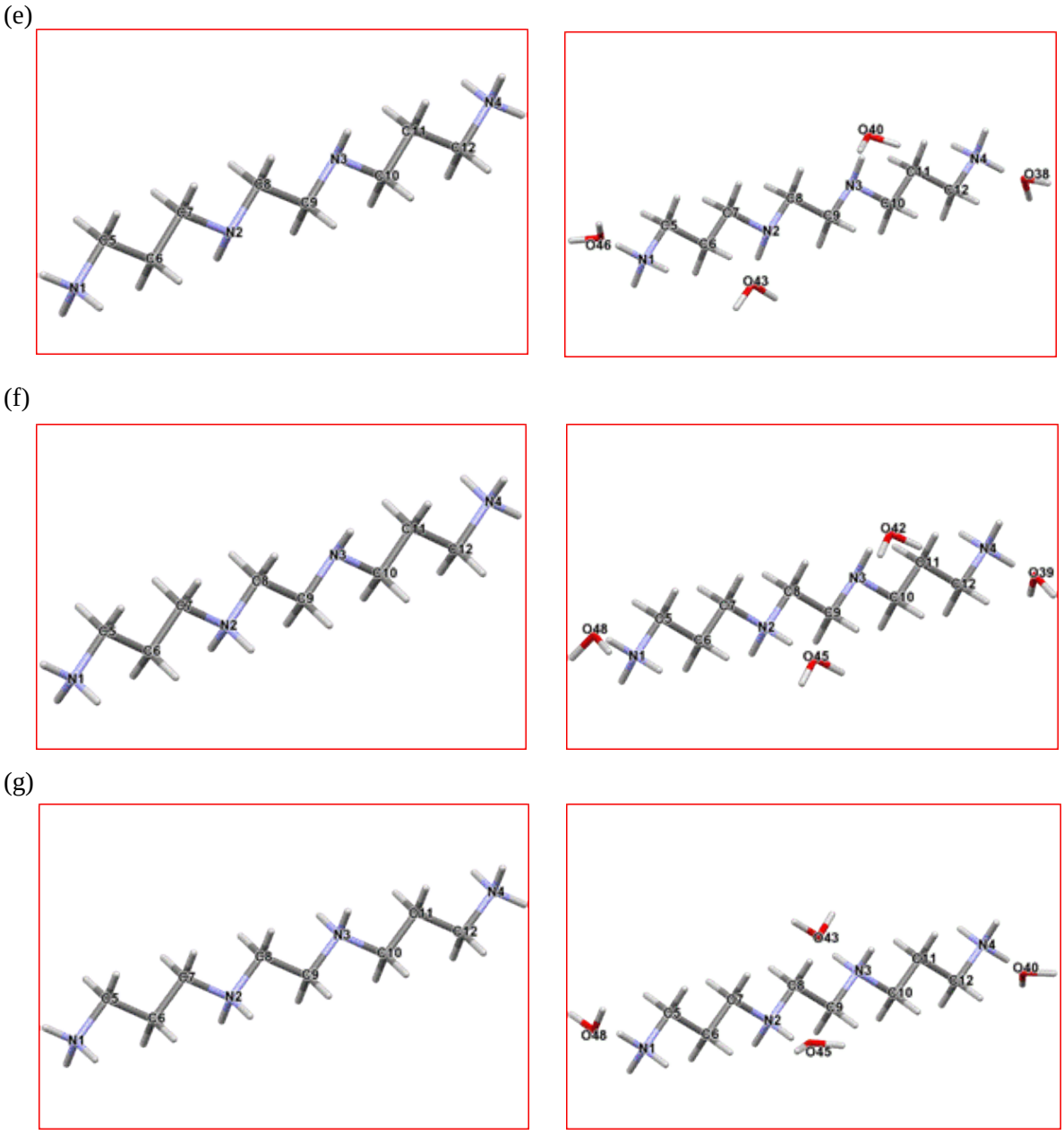

Figure S2. Capped-stick representation of linear structures of H_nL^{n+} forms of 3,2,3-tet with and without explicit water molecules respectively used as inputs for conformational search by MM, also showing atoms' numbering; -part (a) L , -part (b) $HL_{N1}(HL_p)$, -part (c) $HL_{N2}(HL_s)$, part (d) H_2L_{N1N3} (H_2L_{ps}), -part (e) H_2L_{N1N4}(H_2L_{pp}), -part (f) H_3L_{N1N2N4} (H_3L_{psp}) and -part (g) H_4L.

PART 3

Comments on selection of a reference molecule used in the competition reaction

One must realize that it is also necessary to consider the selection of reference molecules in terms of resultant placement of charges among reactants and products. For instance, can one obtain better theoretical estimate of, *e.g.*, (i) the first protonation constant of $L^{(1)}$ using $HL^{(2)}$ or rather $H_2L^{(2)}$ or (ii) the third protonation constants of $H_2L^{(1)}$ involving in the competition reaction $HL^{(2)}$, $H_2L^{(2)}$, $H_3L^{(2)}$, or rather $H_4L^{(2)}$? There is no easy way to predict this and, as an example, see Scheme S1 where (i) both products of the protonation competition reaction have exactly the same charge, (ii) the same number of tautomers for $L^{(1)}$ and $L^{(2)}$ is involved, but (iii) charges on reactants differ. This aspect has also been investigated in the present work in terms of accuracy in the computed protonation constants.

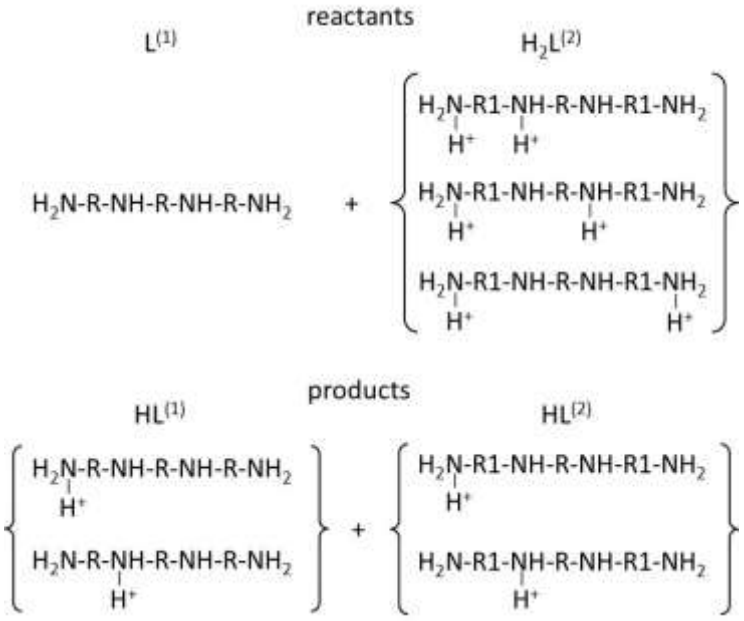

Scheme S1 Possible tautomers of 2,2,2-tet and 3,2,3-tet (R = $–C_2H_4–$; R1 = $–C_3H_6–$) which were considered in the competition reaction based protocol when $L^{(1)}$ and $H_2L^{(2)}$ were employed to compute $\log K_{\mathrm{H}}^{(1)}$ of $L^{(1)}$.

PART 4

Analysis of optimisation profiles

A thorough examination of the optimization profiles of hundreds of 2,2,2-tet conformers fully optimized in Gaussian revealed that there are common patterns when a relationship between electronic energy of a conformer after each optimization cycle and a step number was analysed: (i) a sharp decrease in *E* is observed in the first 3-5 steps in case of conformers which optimise within 10-15 steps; in such a case the relative energies of conformers generally do not change (Figure S3a), (ii) a major decrease in *E* is observed within first 10-15 optimization steps for each conformer and (iii) in many instances a large number of steps was required to reach convergence with insignificant energy change after 20-50*th* step (Figure S3b).

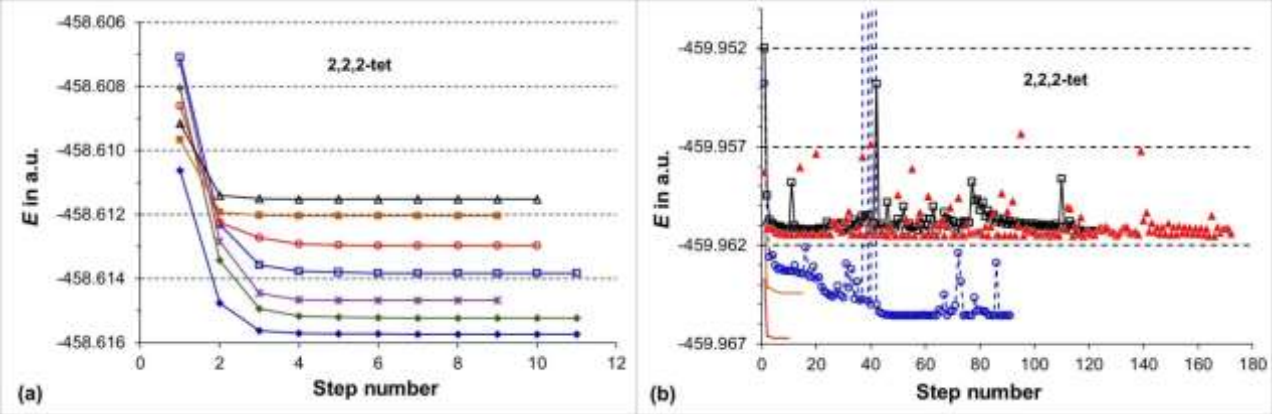

Figure S3. Examples of optimization profiles for selected conformers of 2,2,2-tet in CSM showing the change in the electronic energy *E* with the optimization step in cases of: part (a) - convergence reached within 15 optimization cycles, part (b) - convergence reached after large number of optimization cycles without (red triangles and black squares) and insignificant (blue circles) relative change of conformers' placement in their energy spectrum.

These observations provide a useful hint when one is interested only in the set of the lowest energy conformers needed to compute, *e.g.*, protonation constants; they are discussed in the main body of the text.

PART 5

Lowest energy conformers discovered in the continuum solvation model, PCM.

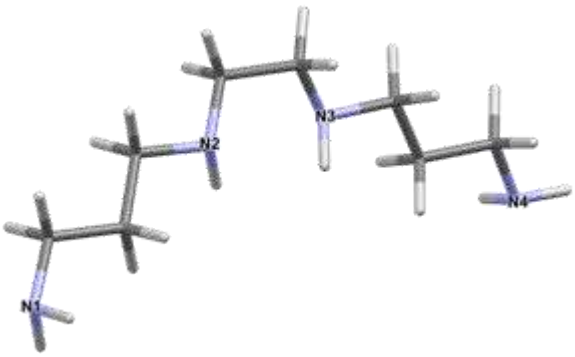

C_L05

C_L02

C_L01

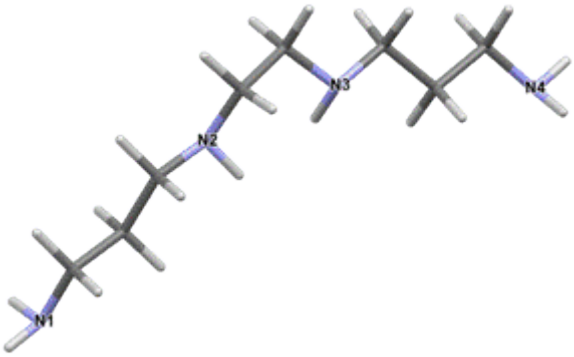

C_L04

C_L06

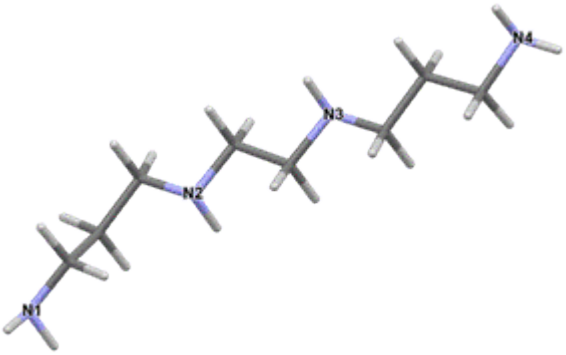

C_L03

Fig. S4. Structures of all lowest in energy conformers of the free ligand of 3,2,3-tet used to calculate protonation constants with continuum solvation model, PCM.

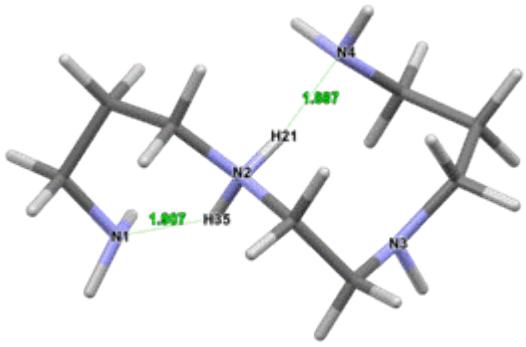

C_s01

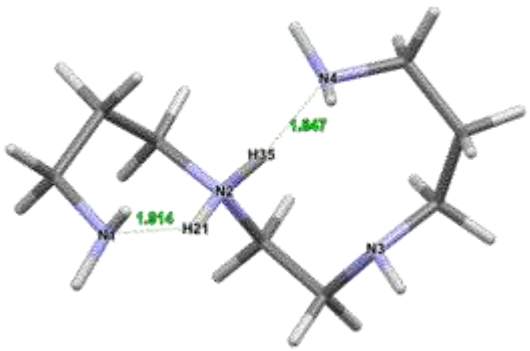

C_s03

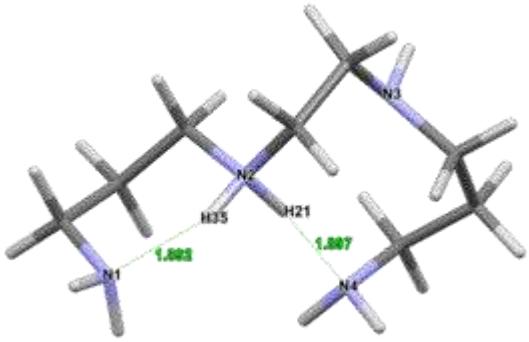

C_s02

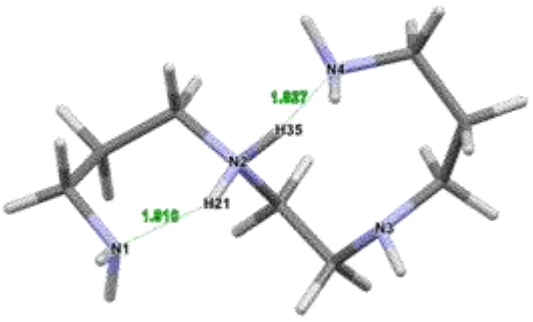

C_s04

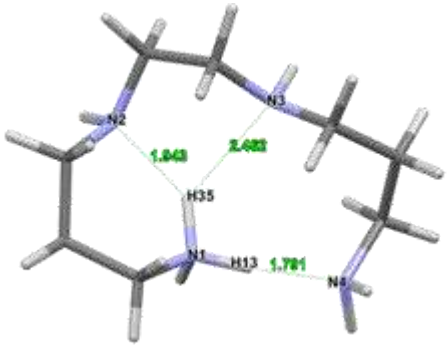

C_p01

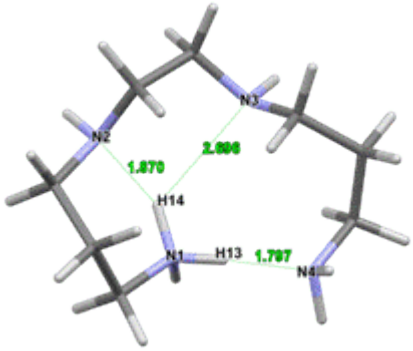

C_p03

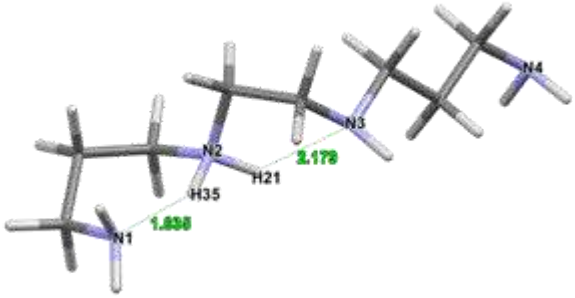

C_s10

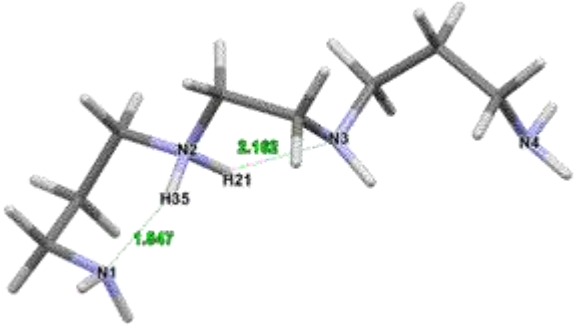

C_s09

Fig. S5. Structures of all lowest in energy conformers for HL form of 3,2,3-tet used to calculate protonation constants with continuum solvation model, PCM

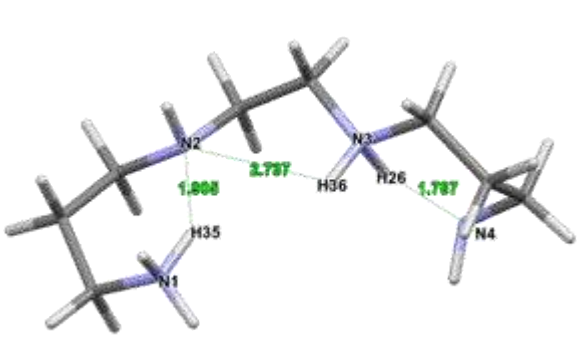

$C_{ps}03$

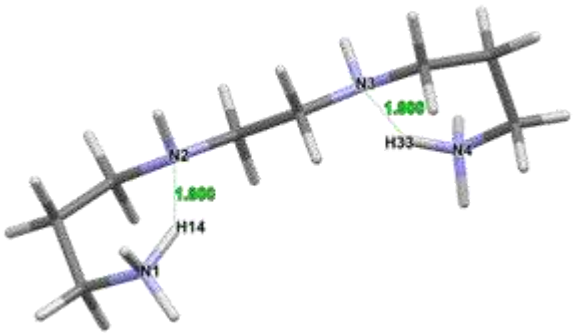

$C_{pp}01$

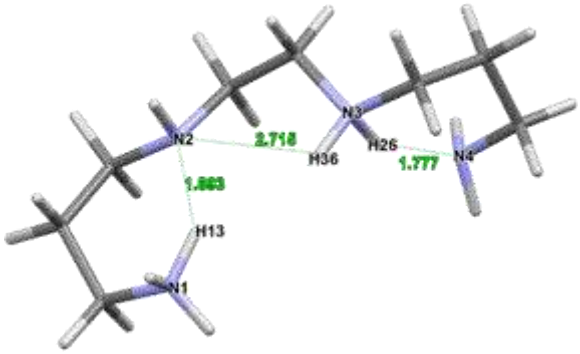

$C_{ps}01$

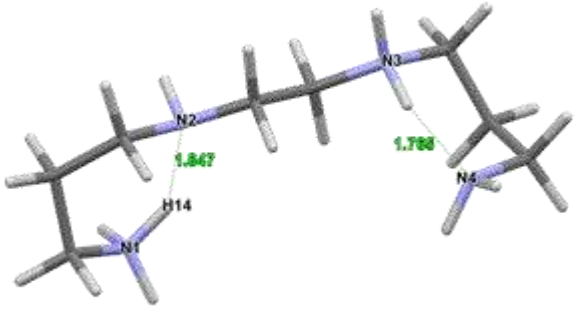

$C_{ps}14$

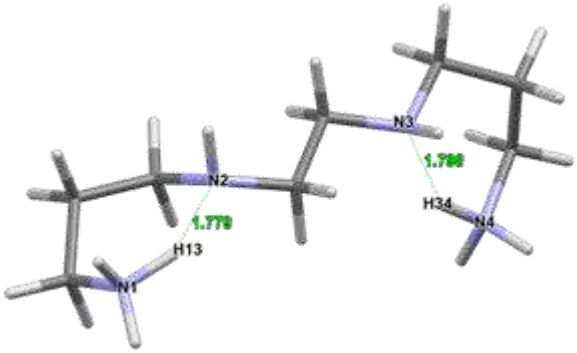

$C_{pp}05$

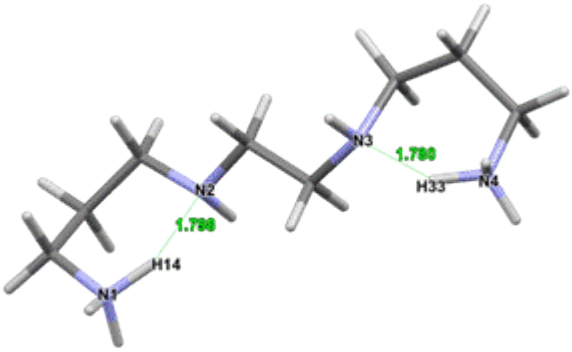

$C_{pp}02$

Fig. S6. Structures of all lowest in energy conformers for H_2L form of 3,2,3-tet used to calculate protonation constants with continuum solvation model, PCM.

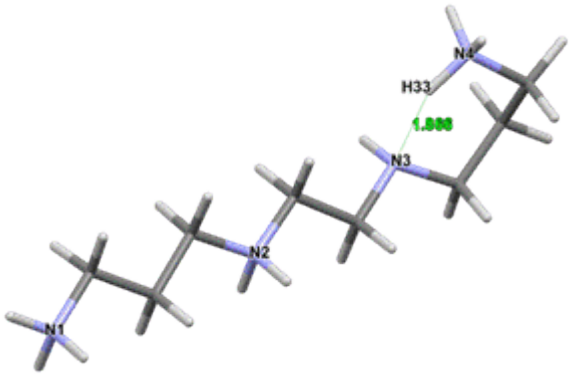

$C_{tp}07$

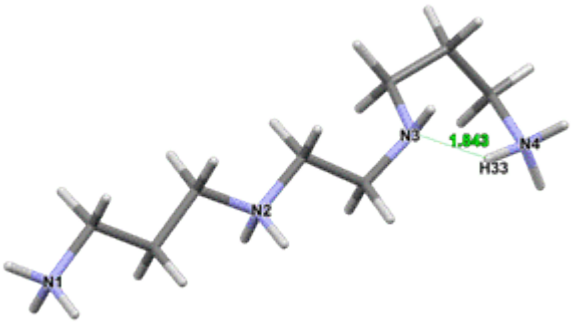

$C_{tp}09$

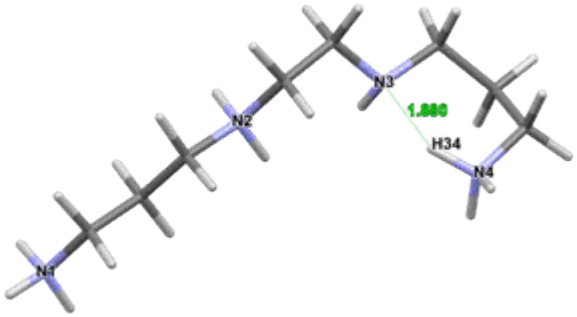

$C_{tp}05$

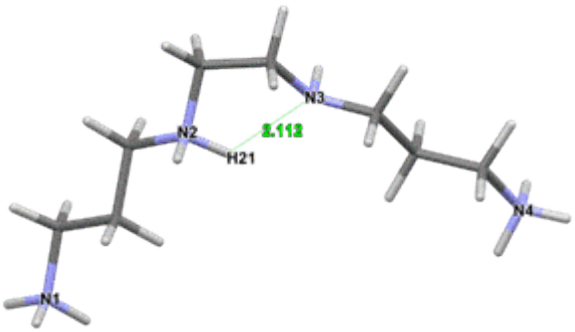

$C_{tp}01$

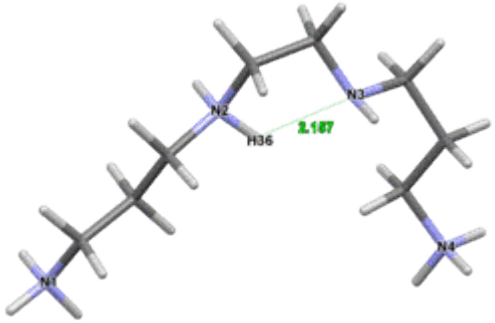

$C_{tp}02$

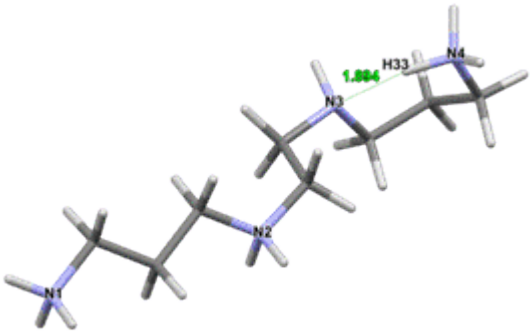

$C_{tp}11$

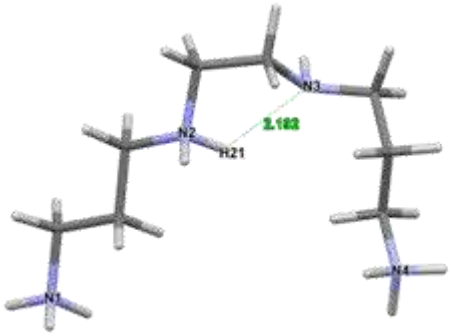

$C_{tp}04$

Fig. S7. Structures of all lowest in energy conformers for H_3L form 3,2,3-tet used to calculate protonation constants with continuum solvation model, PCM.

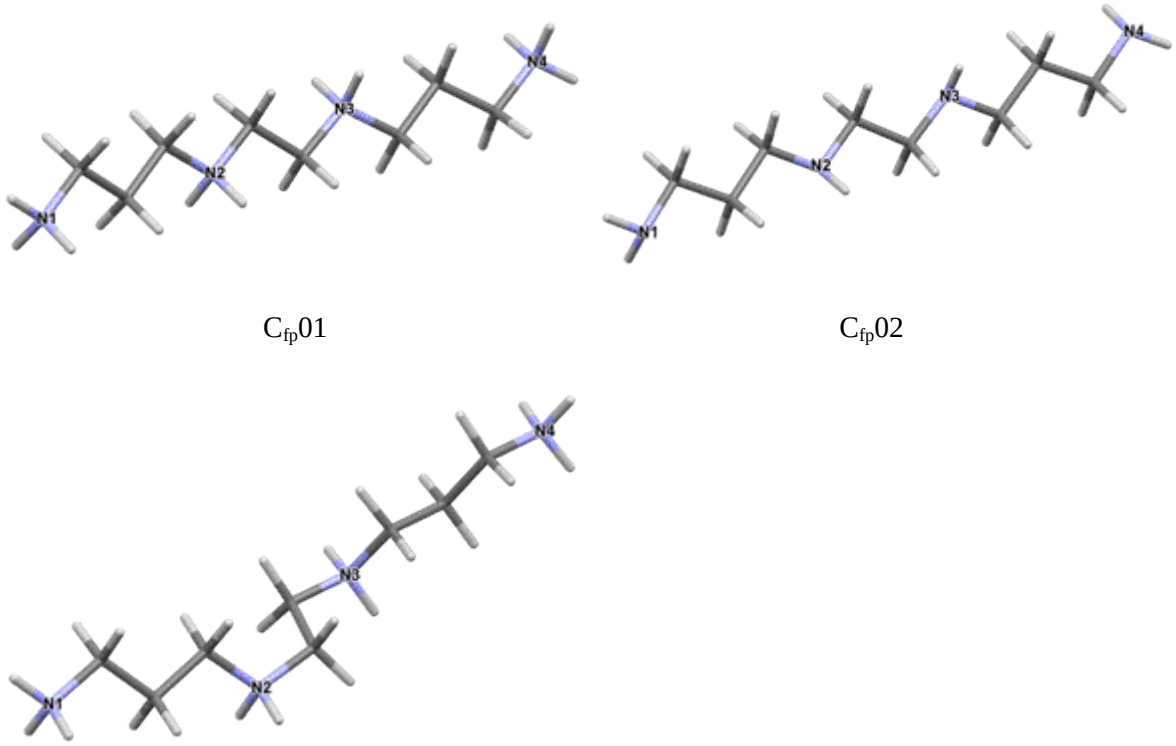

$C_{fp}01$ $C_{fp}02$

$C_{fp}04$

Fig. S8. Structures of all lowest in energy conformers for H_4L form of 3,2,3-tet used to calculate protonation constants with continuum solvation model, PCM.

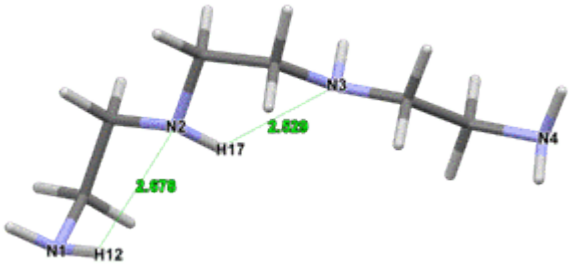

C_L01

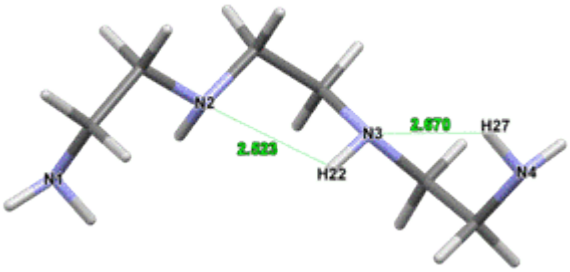

C_L04

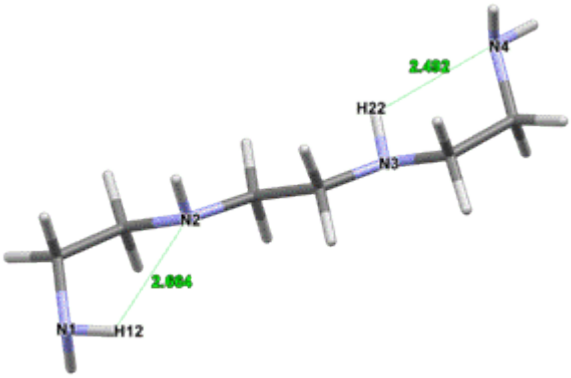

C_L02

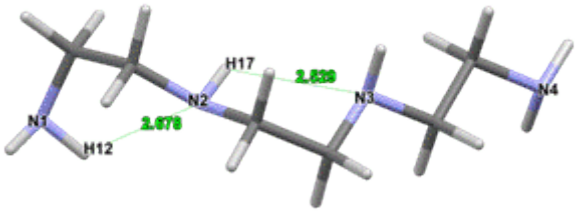

C_L03

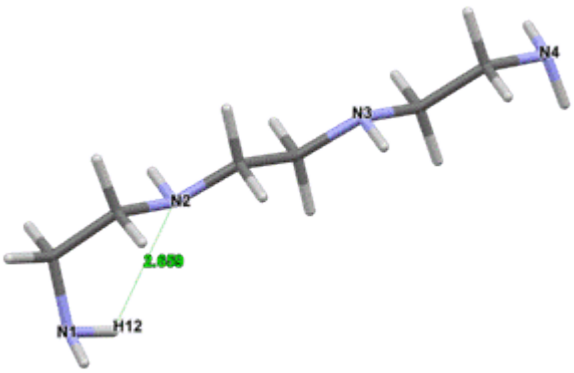

C_L05

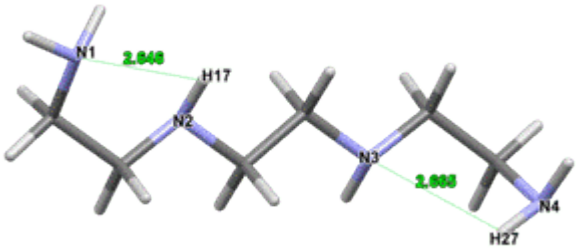

C_L06

Fig. S9. Structures of all lowest in energy conformers for the free ligand of 2,2,2-tet used to calculate protonation constants with continuum solvation model, PCM

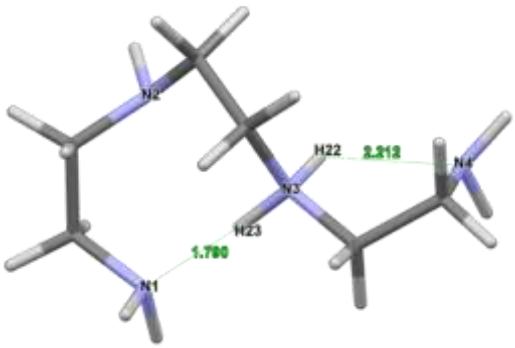

C_s01

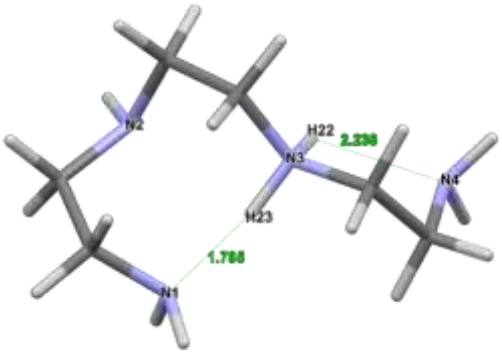

C_s03

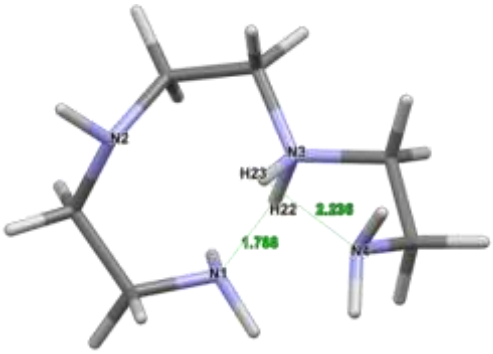

C_s02

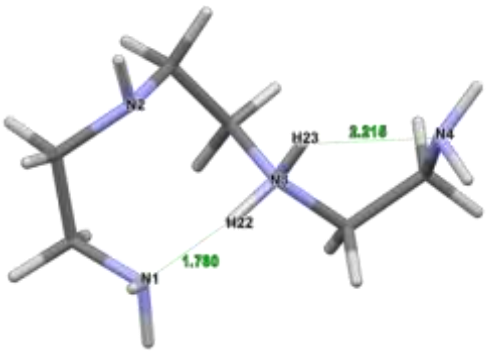

C_s04

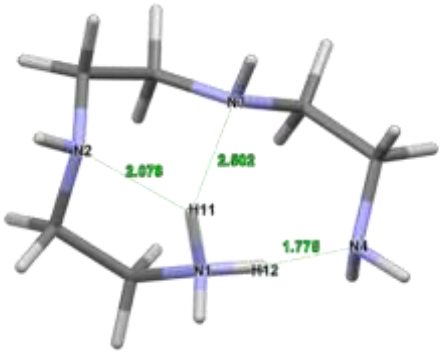

C_p02

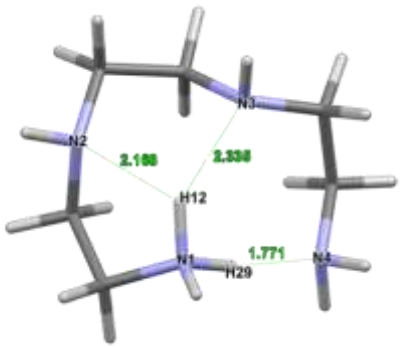

C_p01

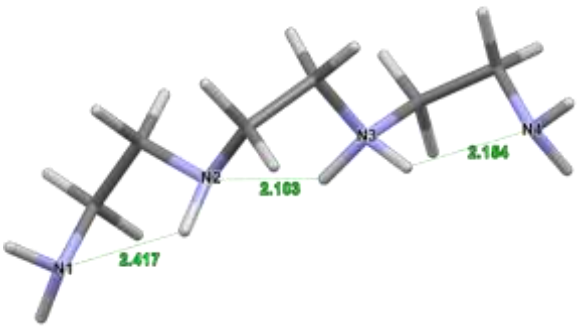

C_s05

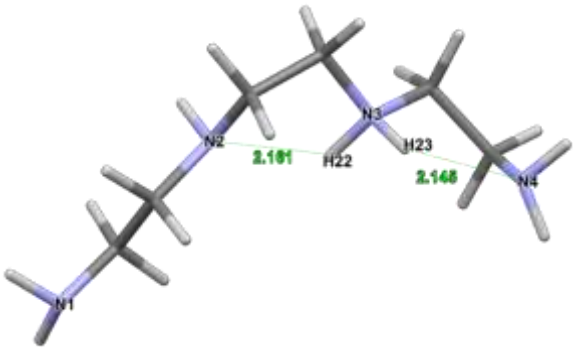

C_s06

Fig. S10. Structures of all lowest in energy conformers for HL form of 2,2,2-tet used to calculate protonation constants with continuum solvation model, PCM.

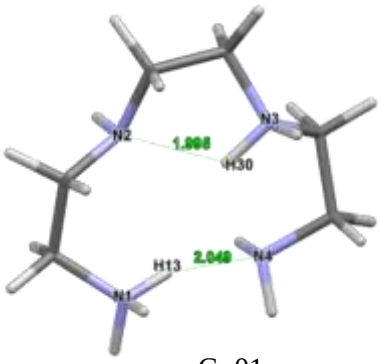

$C_{ps}01$

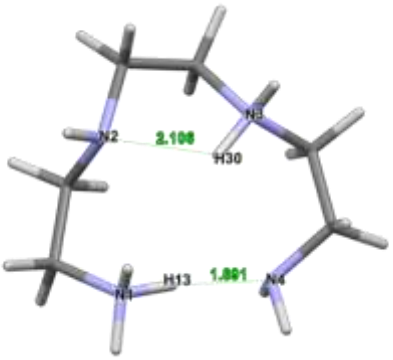

$C_{ps}09$

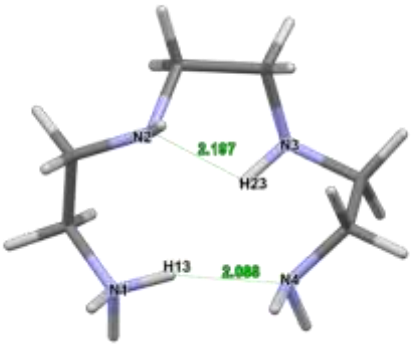

$C_{ps}10$

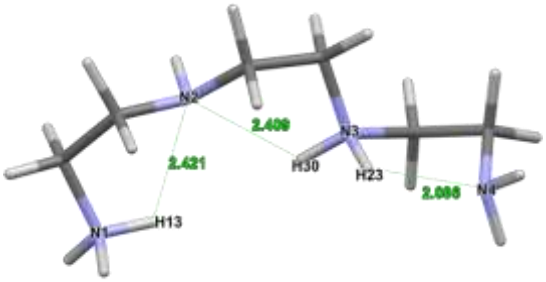

$C_{ps}02$

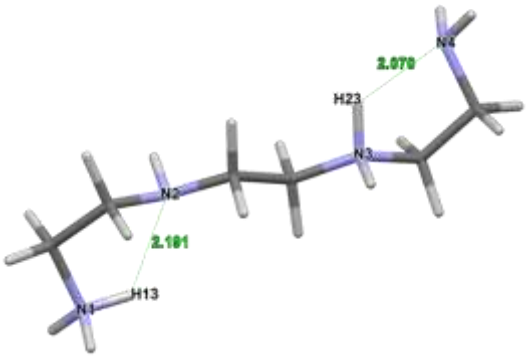

$C_{ps}04$

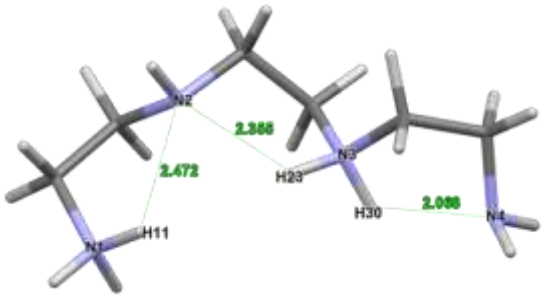

$C_{ps}06$

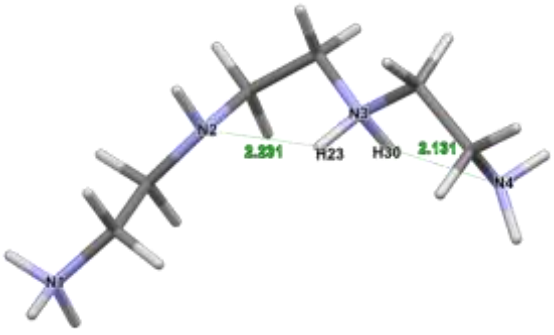

$C_{ps}05$

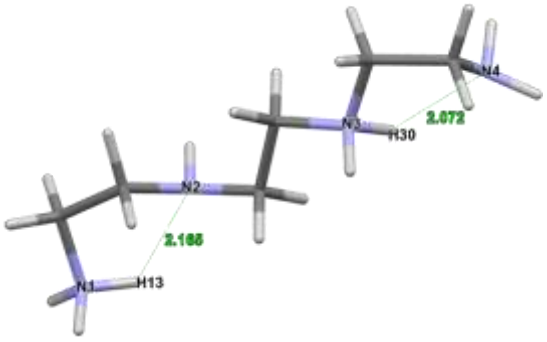

$C_{ps}03$

Fig. S11. Structures of all lowest in energy conformers for H_2L form of 2,2,2-tet used to calculate protonation constants with continuum solvation model, PCM

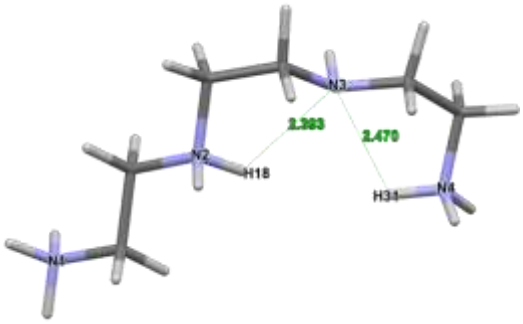

$C_{tp}01$

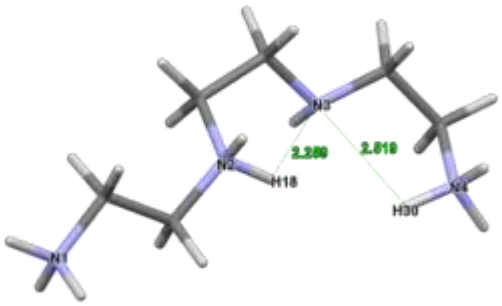

$C_{tp}02$

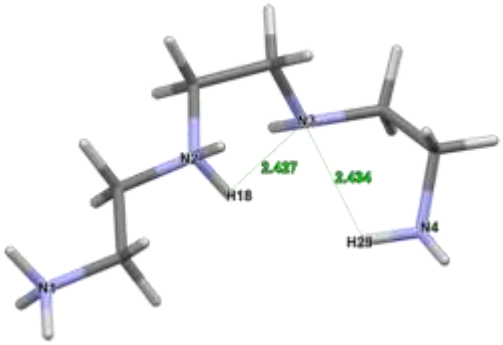

$C_{tp}08$

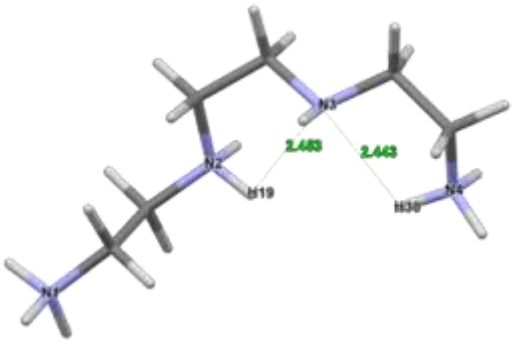

$C_{tp}07$

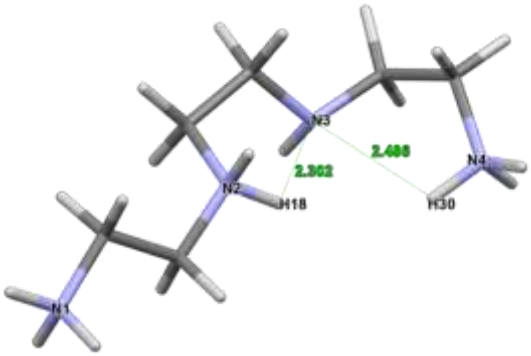

$C_{tp}06$

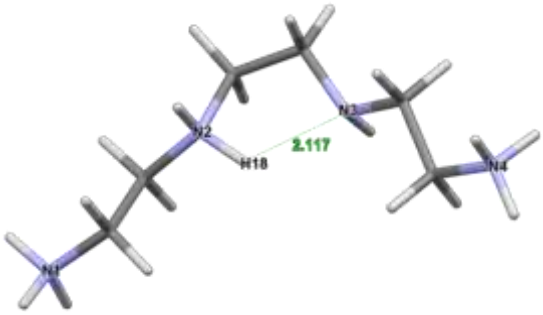

$C_{tp}03$

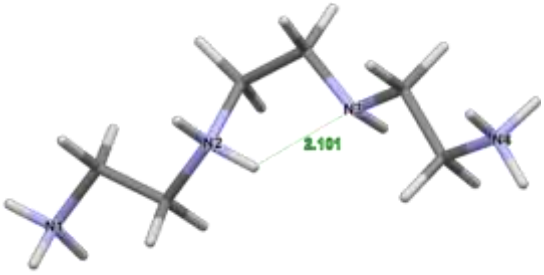

$C_{tp}05$

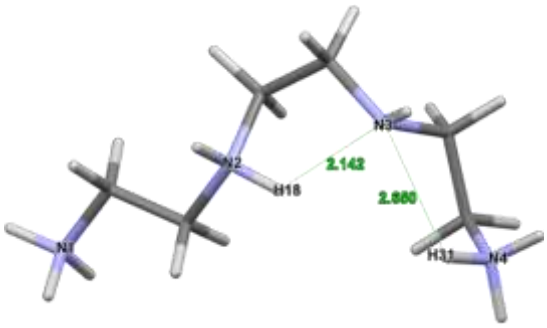

$C_{tp}04$

Fig. S12. Structures of all lowest in energy conformers for H_3L form of 2,2,2-tet used to calculate protonation constants with continuum solvation model, PCM.

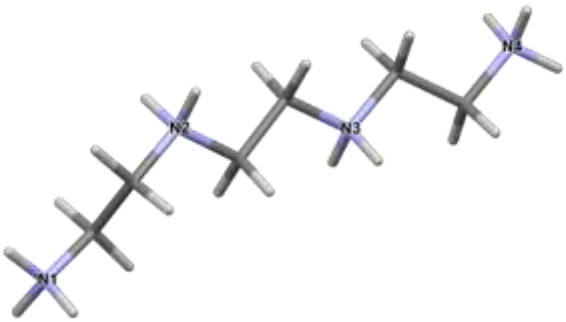

$C_{fp}02$

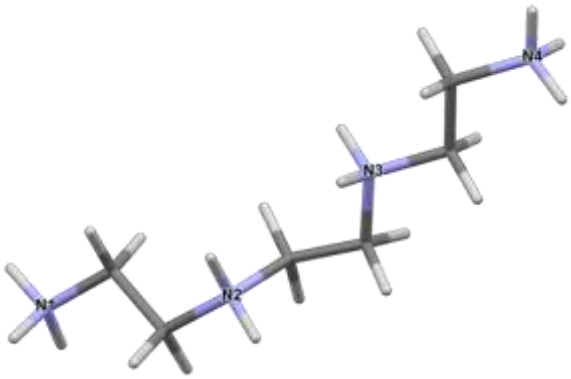

$C_{fp}05$

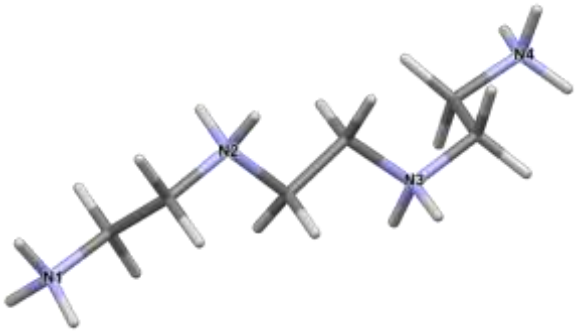

$C_{fp}03$

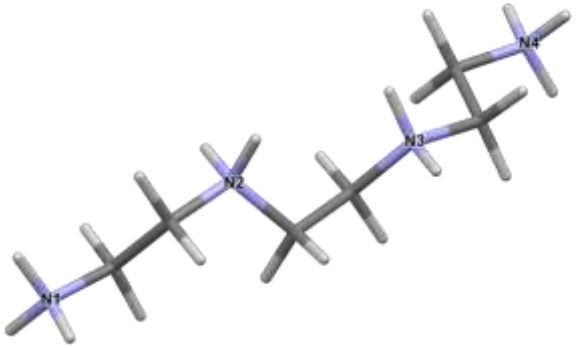

$C_{fp}06$

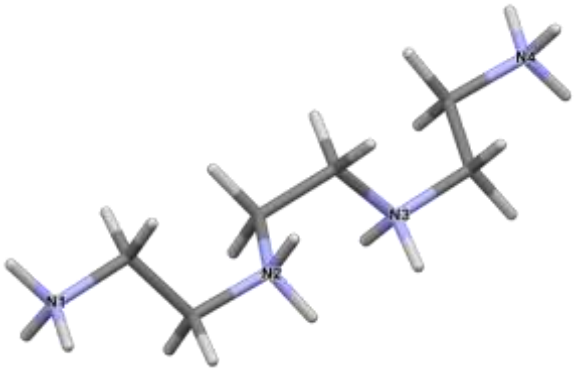

$C_{fp}07$

Fig. S13. Structures of all lowest in energy conformers for H_4L form of 2,2,2-tet used to calculate protonation constants with continuum solvation model, PCM.

PART 6

Lowest energy conformers discovered in the discrete-continuum solvation model.

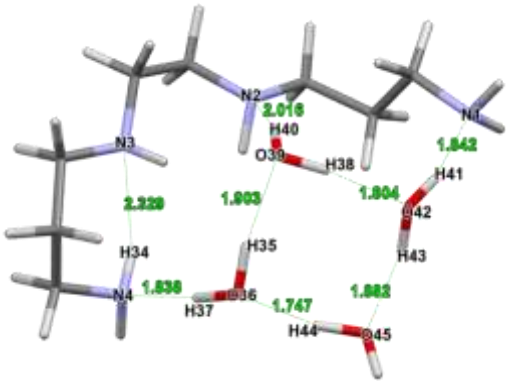

C_L21

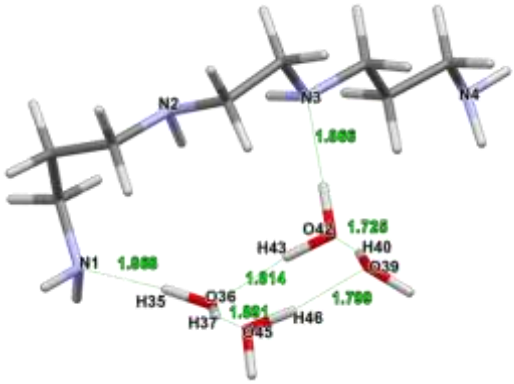

C_L19

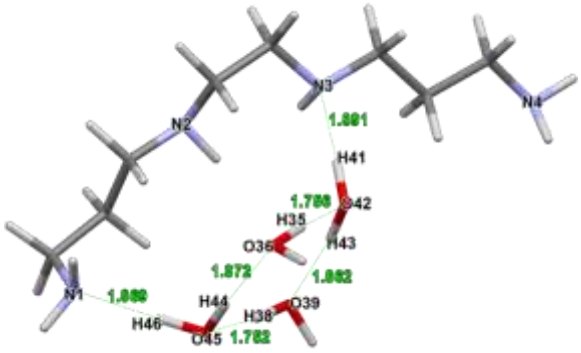

C_L01

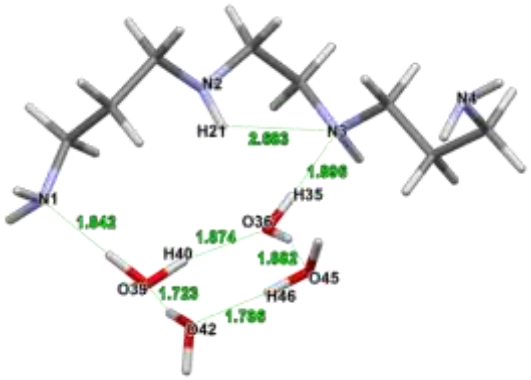

C_L09

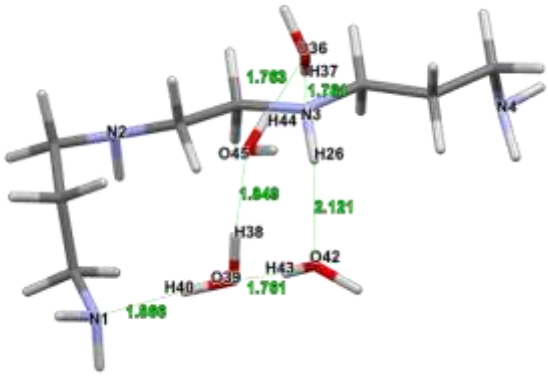

C_L07

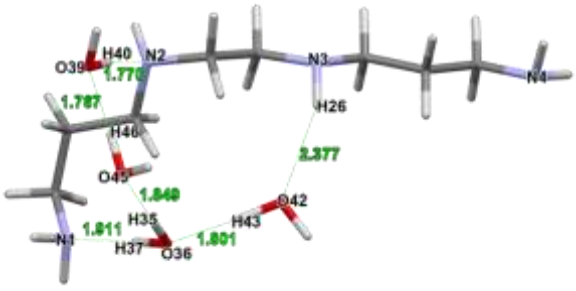

C_L22

Fig. S14. Structures of all lowest in energy conformers of the free ligand of 3,2,3-tet used to calculate protonation constants with discrete-continuum solvation model.

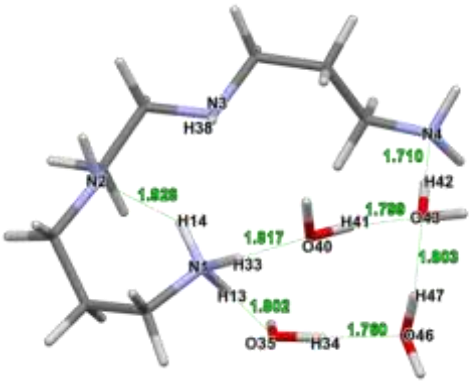

C_p24

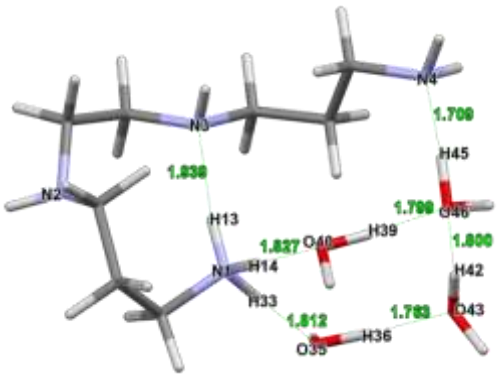

C_p26

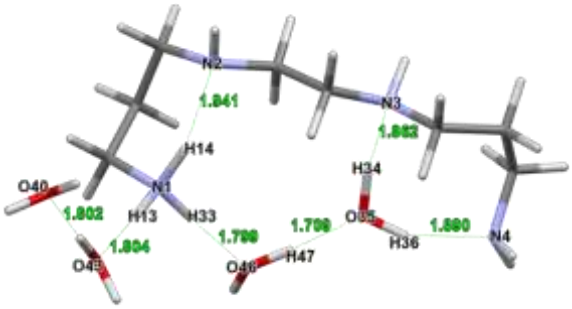

C_p07

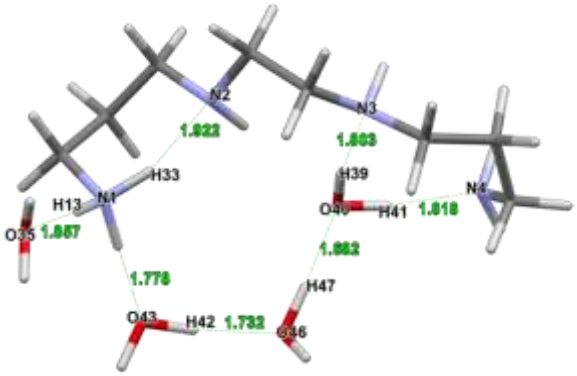

C_p25

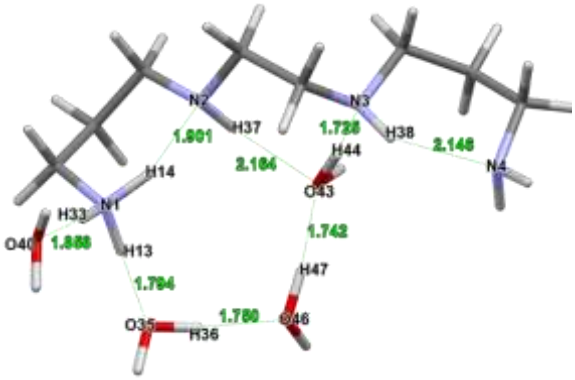

C_p27

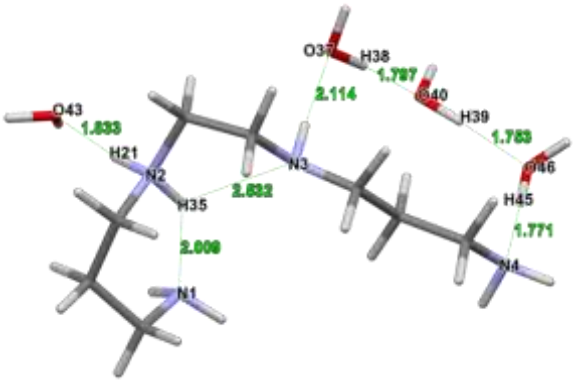

C_s07

Fig. S15. Structures of all lowest in energy conformers for HL form of 3,2,3-tet used to calculate protonation constants with discrete-continuum solvation model.

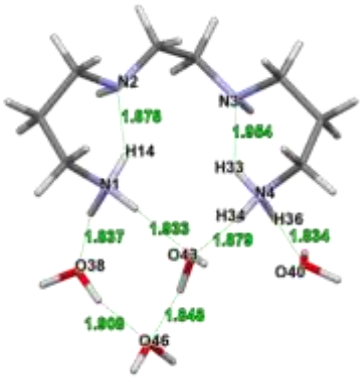

$C_{pp}18$

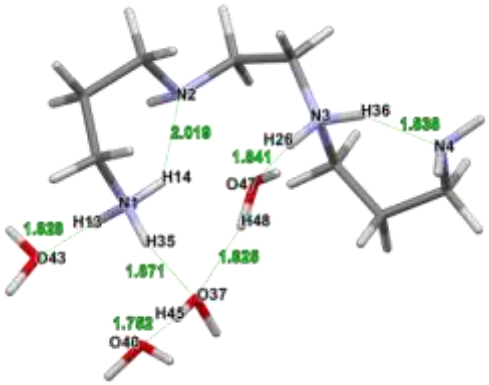

$C_{ps}06$

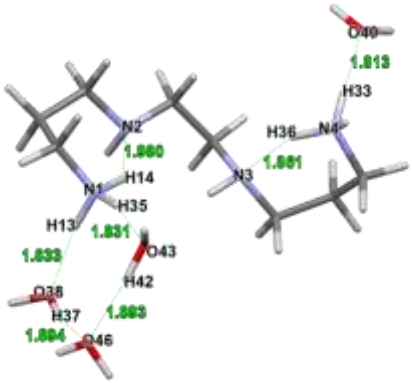

$C_{ps}19$

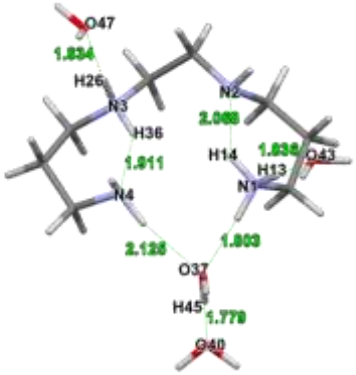

$C_{ps}01$

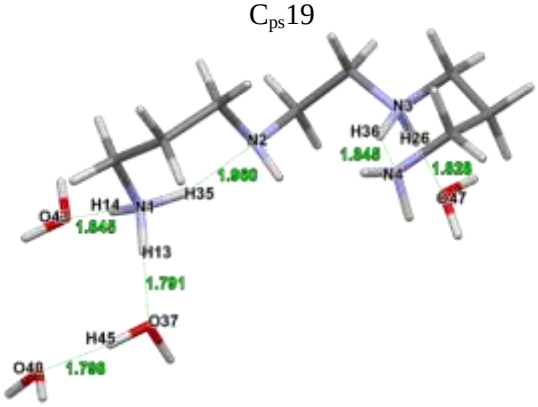

$C_{ps}10$

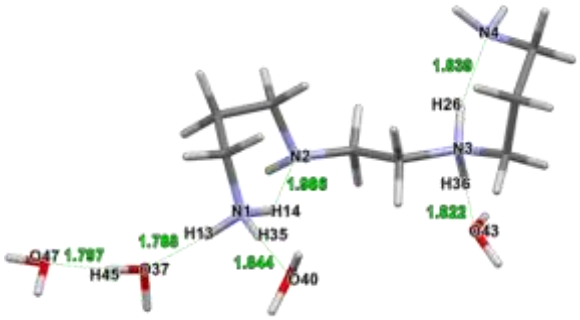

$C_{ps}28$

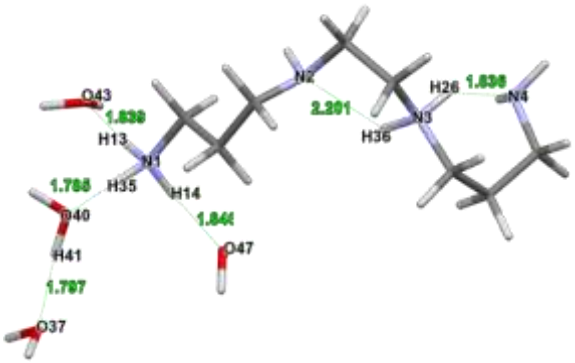

$C_{ps}13$

Fig. S16. Structures of all lowest in energy conformers of H_2L form of 3,2,3-tet used to calculate protonation constants with discrete-continuum solvation model.

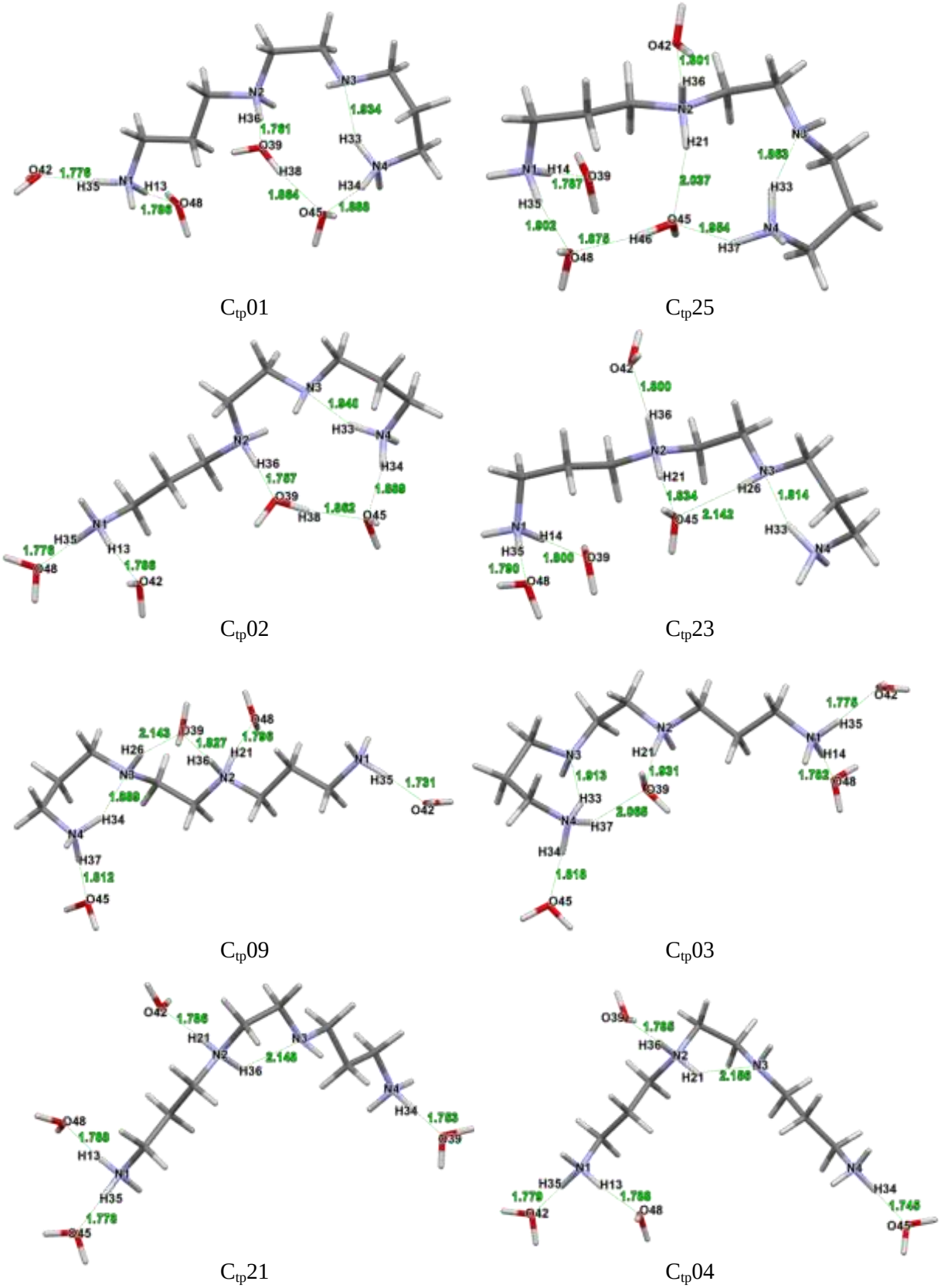

Fig. S17. Structures of all lowest in energy conformers for H_3L form of 3,2,3-tet used to calculate protonation constants with discrete-continuum solvation model.

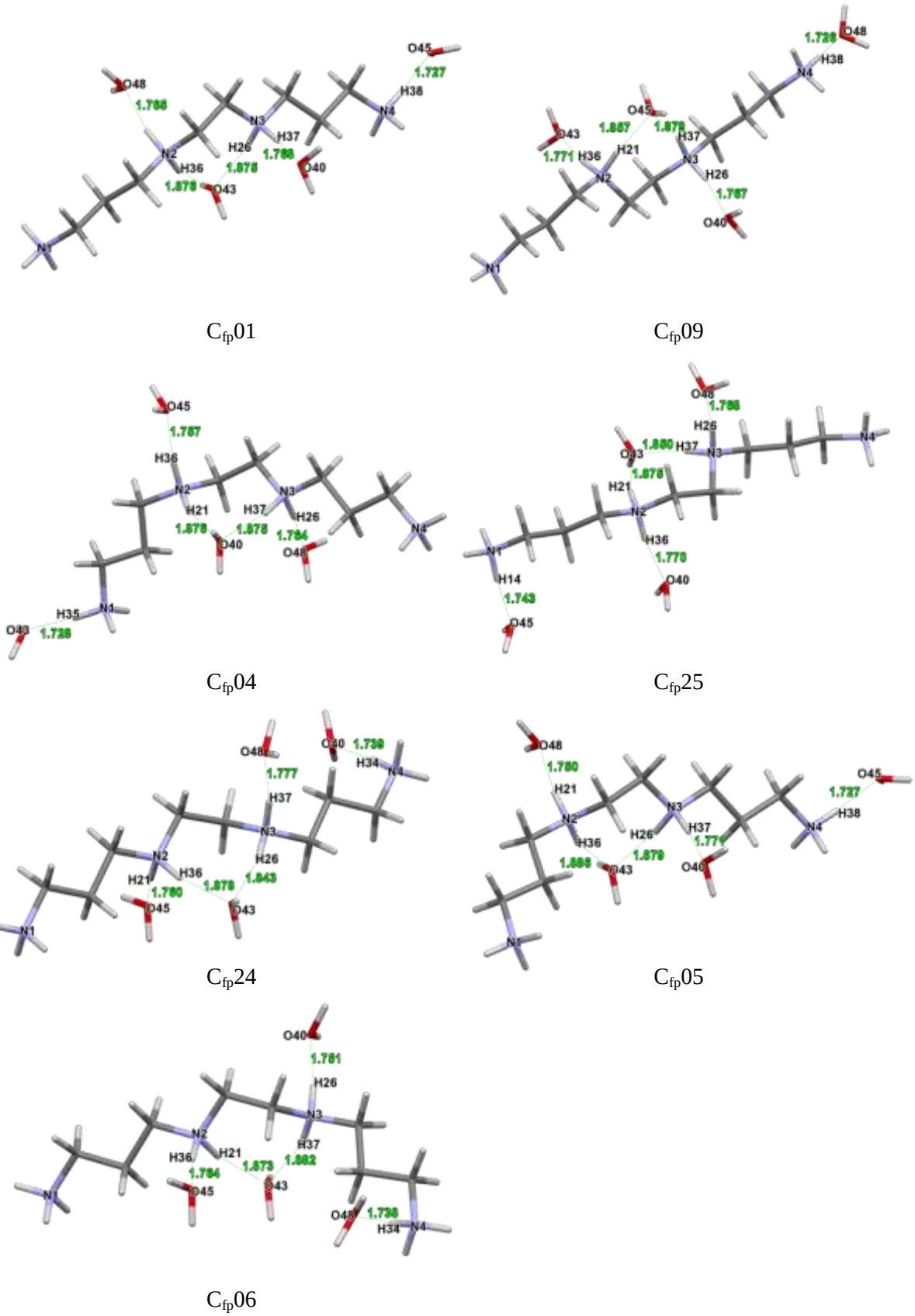

Fig. S18. Structures of all lowest in energy conformers of H_4L form of 3,2,3-tet used to calculate protonation constants with discrete-continuum solvation model.

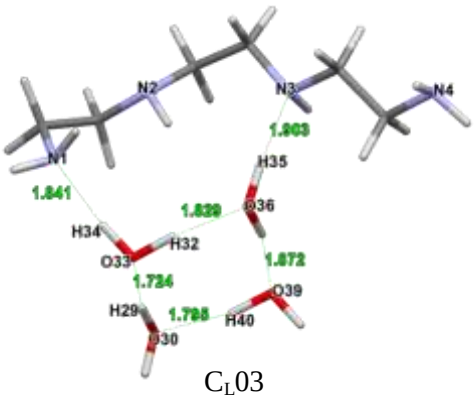

C_L03

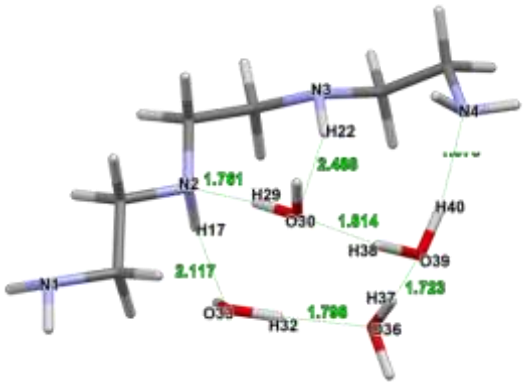

C_L01

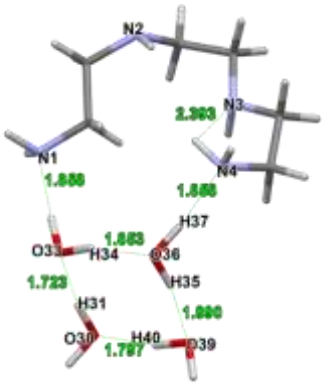

C_L05

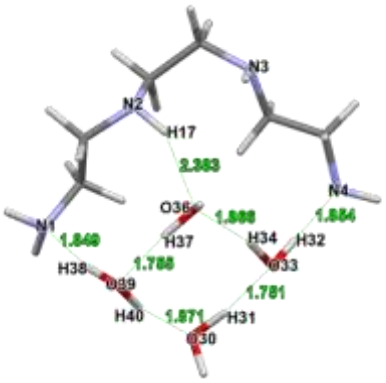

C_L04

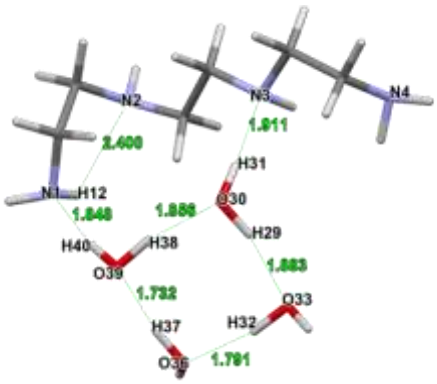

C_L06

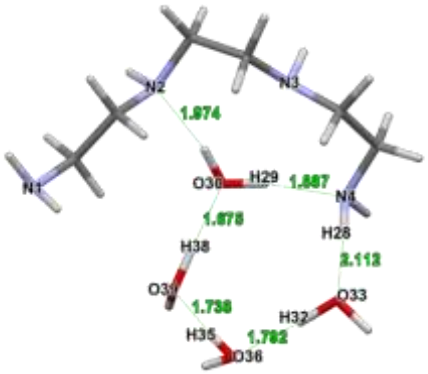

C_L09

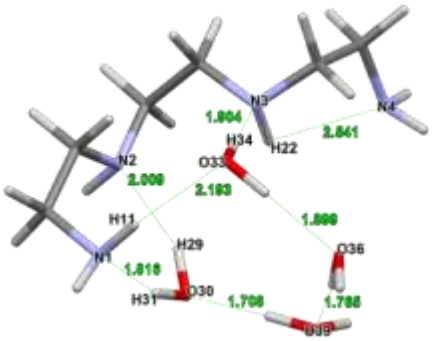

C_L07

Fig. S19. Structures of all lowest in energy conformers of the free Ligand of 2,2,2-tet used to calculate protonation constants with discrete-continuum solvation model.

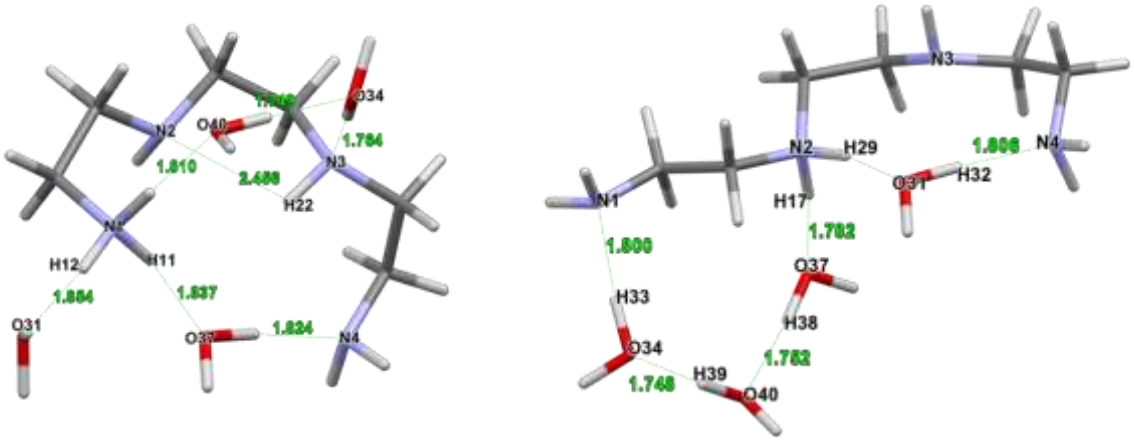

C_p01 C_s07

Fig. S20. Structures of all lowest in energy conformers for HL form of 2,2,2-tet used to calculate protonation constants with discrete-continuum solvation model.

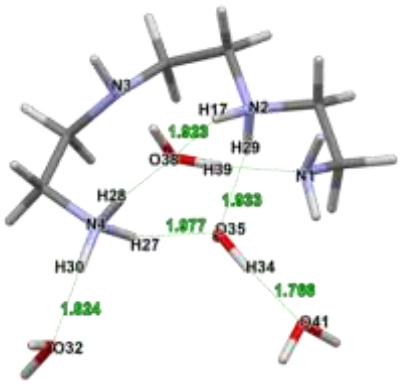

$C_{ps}02$

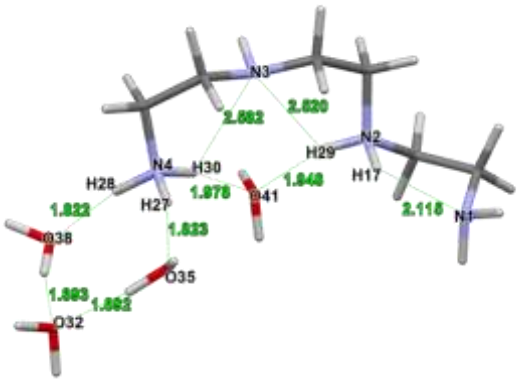

$C_{ps}03$

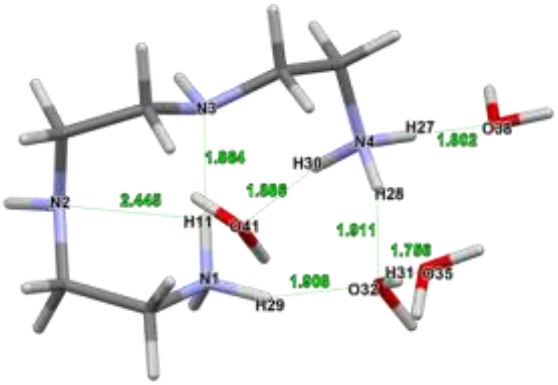

$C_{pp}01$

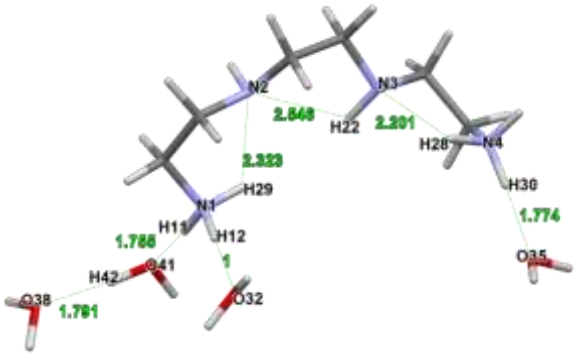

$C_{pp}07$

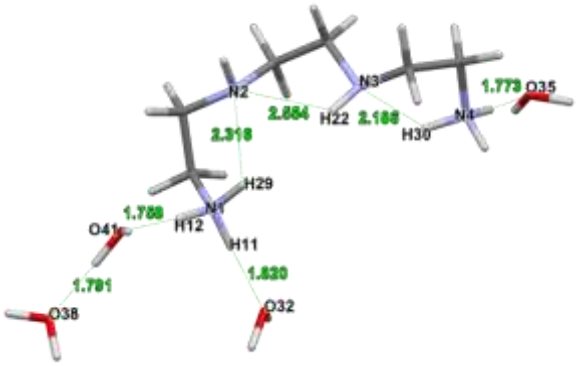

$C_{pp}06$

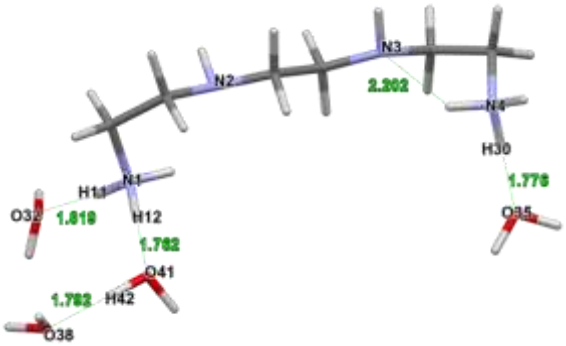

$C_{pp}08$

Fig. S21. Structures of all lowest in energy conformers for H_2L form of 2,2,2-tet used to calculate protonation constants with discrete-continuum solvation model.

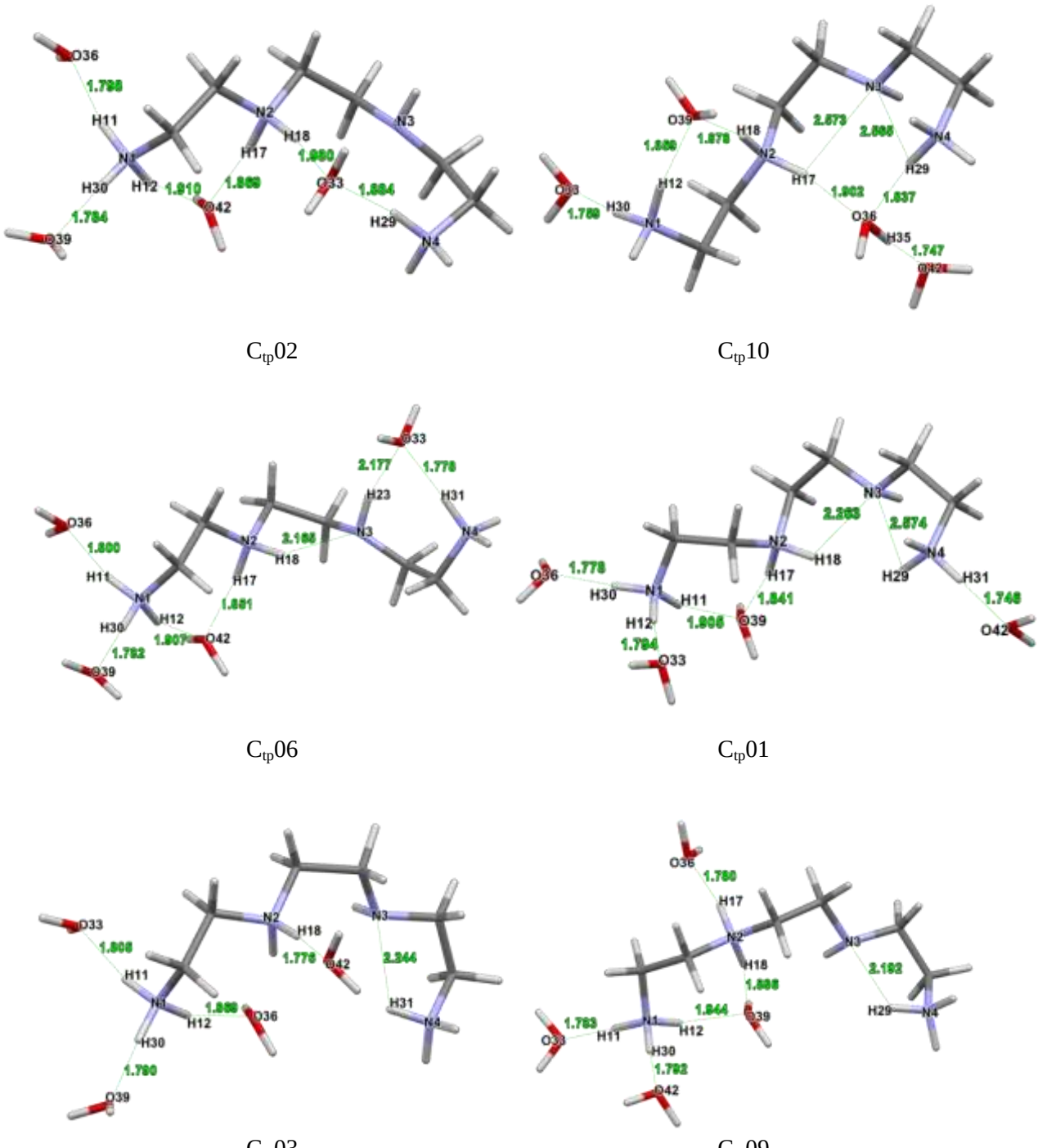

$C_{tp}02$ $C_{tp}10$

$C_{tp}06$ $C_{tp}01$

$C_{tp}03$ $C_{tp}09$

Fig. S22. Structures of all lowest in energy conformers for H_3L form of 2,2,2-tet used to calculate protonation constants with discrete-continuum solvation model.

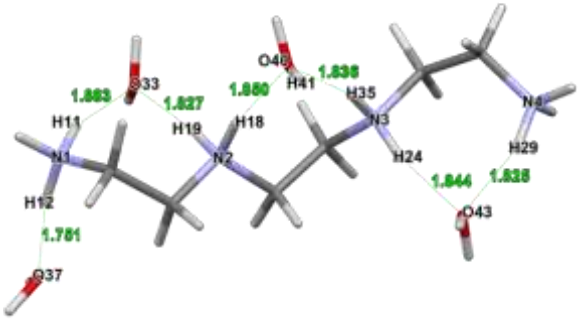

$C_{fp}01$

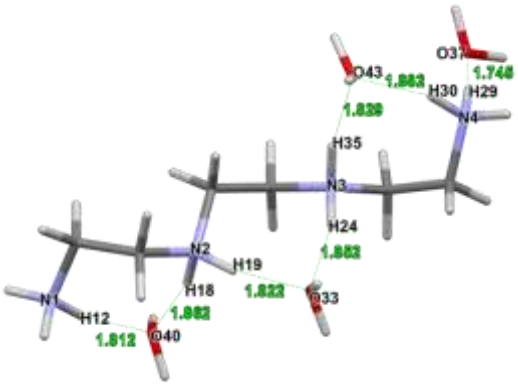

$C_{fp}02$

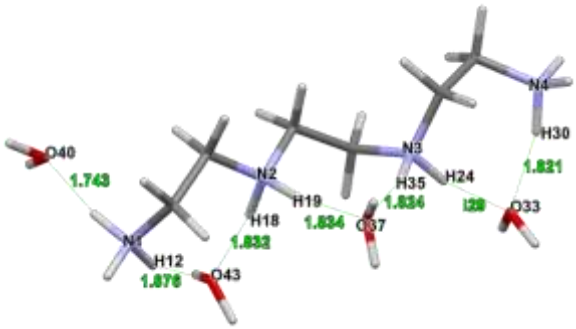

$C_{fp}04$

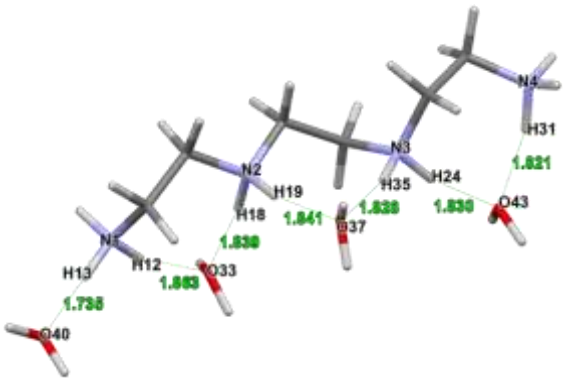

$C_{fp}06$

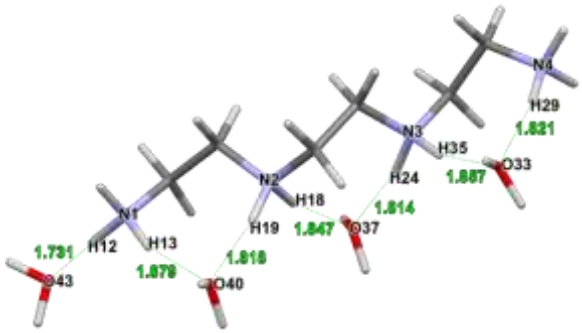

$C_{fp}07$

Fig. S23. Structures of all lowest in energy conformers for H_4L form of 2,2,2-tet used to calculate protonation constants with discrete-continuum solvation model.

Table S1 Five lowest energy conformers of all H_nL in CSM, using either *E* or *G* values, for: part (a) 2,2,2-tet and part (b) 3,2,3-tet.[a]

(a)

L			HL			H_2L			H_3L			H_4L		
Conf	Δ*E*	%	Conf	Δ*E*	%	Conf	Δ*E*	%	Conf	Δ*E*	%	Conf	Δ*E*	%
$C_{fL}01$	0.00	18.83	C_s01	0.00	41.41	$C_{ps}01$	0.00	60.29	$C_{tp}01$	0.00	81.22	$C_{fp}02$	0.00	92.70
$C_{fL}02$	0.21	13.30	C_s02	0.29	25.38	$C_{ps}02$	0.33	34.45	$C_{tp}02$	1.23	10.14	$C_{fp}05$	1.50	7.30
$C_{fL}03$	0.29	11.54	C_s03	0.46	19.16	$C_{ps}09$	1.79	2.95	$C_{tp}03$	1.81	3.85			
$C_{fL}04$	0.43	9.15	C_s04	0.82	10.34	$C_{ps}10$	1.93	2.31	$C_{tp}06$	2.36	1.51			
$C_{fL}05$	0.77	5.14	C_p01	2.07	1.27				$C_{tp}07$	2.48	1.23			
Conf	Δ*G*	%	Conf	Δ*G*	%	Conf	Δ*G*	%	Conf	Δ*G*	%	Conf	Δ*G*	%
$C_{fL}01$	0.00	18.57	C_s01	0.00	30.94	$C_{ps}01$	0.00	33.04	$C_{tp}01$	0.00	75.05	$C_{fp}02$	0.00	72.57
$C_{fL}02$	0.21	13.12	C_s02	0.29	18.96	$C_{ps}02$	0.33	18.88	$C_{tp}02$	1.23	9.37	$C_{fp}03$	0.72	21.34
$C_{fL}03$	0.29	11.38	C_s03	0.46	14.32	$C_{ps}03$	0.49	14.35	$C_{tp}03$	1.81	3.56	$C_{fp}05$	1.50	5.72
$C_{fL}04$	0.43	9.02	C_s04	0.82	7.73	$C_{ps}04$	0.88	7.42	$C_{tp}04$	1.99	2.59	$C_{fp}06$	3.40	0.23
$C_{fL}05$	0.77	5.06	C_s05	0.88	6.97	$C_{ps}05$	1.40	3.13	$C_{tp}05$	2.28	1.59	$C_{fp}07$	3.69	0.14

(b)

L			HL			H_2L			H_3L			H_4L		
Conf	Δ*E*	%	Conf	Δ*E*	%	Conf	Δ*E*	%	Conf	Δ*E*	%	Conf	Δ*E*	%
$C_{fL}01$	0.00	25.74	C_s03	0.00	42.00	$C_{ps}14$	0.00	28.34	$C_{tp}02$	0.00	40.47	$C_{fp}01$	0.00	96.41
$C_{fL}05$	0.21	17.95	C_s01	0.19	30.72	$C_{ps}03$	0.04	26.59	$C_{tp}07$	0.30	24.41	$C_{fp}02$	1.95	3.59
$C_{fL}02$	0.40	13.08	C_s02	0.74	11.95	$C_{pp}01$	0.60	10.21	$C_{tp}01$	0.47	18.40			
$C_{fL}06$	0.81	6.54	C_s04	0.75	11.78	$C_{pp}05$	0.73	8.21	$C_{tp}09$	0.67	12.97			
$C_{fL}03$	0.83	6.36	C_p01	1.72	2.29	$C_{pp}02$	0.99	5.29	$C_{tp}05$	1.62	2.60			
Conf	Δ*G*	%	Conf	Δ*G*	%	Conf	Δ*G*	%	Conf	Δ*G*	%	Conf	Δ*G*	%
$C_{fL}01$	0.00	25.52	C_s03	0.00	35.93	$C_{ps}14$	0.00	27.69	$C_{tp}02$	0.00	39.93	$C_{fp}01$	0.00	96.32
$C_{fL}05$	0.21	17.80	C_s01	0.19	26.29	$C_{ps}03$	0.04	25.98	$C_{tp}07$	0.30	24.09	$C_{fp}02$	1.95	3.59
$C_{fL}02$	0.40	12.97	C_s02	0.74	10.23	$C_{pp}01$	0.60	9.98	$C_{tp}01$	0.47	18.15	$C_{fp}04$	4.15	0.09
$C_{fL}06$	0.81	6.49	C_s04	0.75	10.07	$C_{pp}05$	0.73	8.02	$C_{tp}09$	0.67	12.79			
$C_{fL}03$	0.83	6.31	C_s10	0.99	6.73	$C_{pp}02$	0.99	5.17	$C_{tp}05$	1.62	2.57			

[a]Conf stands for conformer; Δ*E* (Δ*G*) was calculated relative to the lowest *E* (*G*) energy conformer; % is the %-fraction of the total population from Boltzmann distribution.

Table S2. Examples of competition reactions in which reference molecule used had either smaller or larger, or similar number of protons relative to the molecule being investigated.

Reaction	$\log K_H^{(n)}$	Δ
$HL^{(1)} + HL^{(2)} = H_2L^{(1)} + L^{(2)}$	15.56	6.56
$H_2L^{(1)} + HL^{(2)} = H_3L^{(1)} + L^{(2)}$	15.47	8.89
$H_3L^{(1)} + HL^{(2)} = H_4L^{(1)} + L^{(2)}$	14.33	11.06
$L^{(1)} + H_2L^{(2)} = HL^{(1)} + HL^{(2)}$	3.01	–6.74
$H_2L^{(1)} + H_2L^{(2)} = H_3L^{(1)} + HL^{(2)}$	8.72	2.14
$H_3L^{(1)} + H_2L^{(2)} = H_4L^{(1)} + HL^{(2)}$	7.58	4.31

Δ = computed – experimental $\log K_H^{(n)}$

Table S3. Computed from *E*- and *G*-paths protonation constants, as $\log K_H^{(n)}$, for 2,2,2-tet using data from dispersion corrected DFT in a discrete-continuum solvation model using B3LYP-gD3 in part(a) and B97D in part (b).[a]

(a)

	***E*-path**				
	***G* of LEC**		**Weighted *G***		
Reaction	$\log K_H^{(n)}$	Δ_1	$\log K_H^{(n)}$	Δ_2	$\Delta_1 - \Delta_2$
$L^{(1)} + HL^{(2)} = HL^{(1)} + L^{(2)}$	11.45	1.70	11.34	1.59	0.11
$HL^{(1)} + H_2L^{(2)} = H_2L^{(1)} + HL^{(2)}$	10.30	1.23	10.47	1.40	0.17
$H_2L^{(1)} + H_3L^{(2)} = H_3L^{(1)} + H_2L^{(2)}$	5.63	–0.95	5.37	–1.21	0.26
$H_3L^{(1)} + H_4L^{(2)} = H_4L^{(1)} + H_3L^{(2)}$	1.98	–1.29	2.14	–1.13	0.16
	***G*-path**				
	***G* of LEC**		**Weighted *G***		
$L^{(1)} + HL^{(2)} = HL^{(1)} + L^{(2)}$	11.45	-1.70	11.62	-1.87	0.17
$HL^{(1)} + H_2L^{(2)} = H_2L^{(1)} + HL^{(2)}$	9.27	-0.20	9.21	-0.14	0.06
$H_2L^{(1)} + H_3L^{(2)} = H_3L^{(1)} + H_2L^{(2)}$	6.66	-0.08	6.68	-0.10	0.02
$H_3L^{(1)} + H_4L^{(2)} = H_4L^{(1)} + H_3L^{(2)}$	1.98	1.29	2.00	1.27	0.02

(b)

	***E*-path**				
	***G* of LEC**		**Weighted *G***		
Reaction	$\log K_H^{(n)}$	Δ_1	$\log K_H^{(n)}$	Δ_2	$\Delta_1 - \Delta_2$
$L^{(1)} + HL^{(2)} = HL^{(1)} + L^{(2)}$	10.56	–0.81	11.34	–1.59	0.78
$HL^{(1)} + H_2L^{(2)} = H_2L^{(1)} + HL^{(2)}$	9.78	–0.71	10.47	–1.40	0.69
$H_2L^{(1)} + H_3L^{(2)} = H_3L^{(1)} + H_2L^{(2)}$	6.30	0.28	5.37	1.21	0.93
$H_3L^{(1)} + H_4L^{(2)} = H_4L^{(1)} + H_3L^{(2)}$	2.12	1.15	2.14	1.13	0.02
	***G*-path**				
	***G* of LEC**		**Weighted *G***		
$L^{(1)} + HL^{(2)} = HL^{(1)} + L^{(2)}$	10.56	–0.81	10.85	–1.10	0.29
$HL^{(1)} + H_2L^{(2)} = H_2L^{(1)} + HL^{(2)}$	8.89	0.18	8.97	0.10	0.08
$H_2L^{(1)} + H_3L^{(2)} = H_3L^{(1)} + H_2L^{(2)}$	7.18	–0.60	7.03	–0.45	0.15
$H_3L^{(1)} + H_4L^{(2)} = H_4L^{(1)} + H_3L^{(2)}$	2.12	1.15	1.92	–1.35	0.20

[a]Weighted *G* values were obtained using each conformers fraction of the total population (from Boltzmann distribution) as a weight for their *G* contribution ($w \times G$); Δ_n = computed – experimental $\log K_H^{(n)}$.

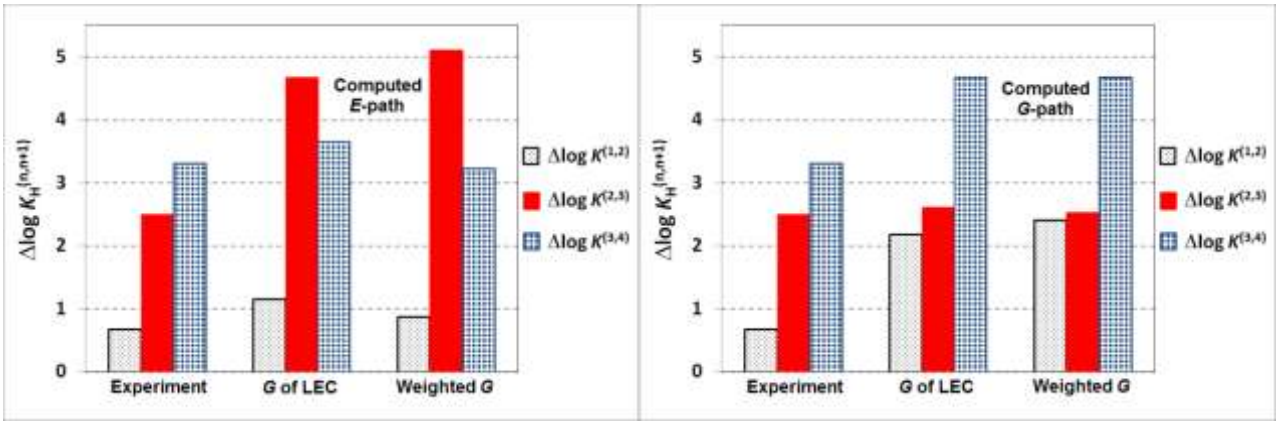

Figure S24. Graphical presentation of differences between successive stepwise protonation constants, $\Delta\log K^{(n,n+1)} = \log K_H^{(n)} - \log K_H^{(n+1)}$, for computed data at the B3LYP-gD3 level of theory with DCSM (values obtained for experimental data is also included for comparison).

Table S4. Summary of identified (yes) and missed (no) lowest energy conformers of 2,2,2-tet and 3,2,3-tet in DCSM from proposed the pre-optimization protocol involving selection of conformers after 20 optimization steps with 4 kcal/mol *E*-window showing also an impact on computed protonation constants.[a]

	2,2,2-tet		3,2,3-tet		F-set	R-set	F-set	R-set
Prot. form	**The LEC**	**LECs**	**The LEC**	**LECs**	**log $K_H^{(2)}$**	**log $K_H^{(2)}$**	**log $K_H^{(3)}$**	**log $K_H^{(3)}$**
L	yes	yes	yes	yes	–	–	–	–
HL_p	yes	yes	yes	yes	–	–	–	–
HL_s	yes	yes	yes	yes	–	–	–	–
H_2L_{ps}	yes	no (1)*	yes	yes	8.68	8.75	6.25	6.19
H_2L_{pp}	yes	yes	yes	yes	–	–	–	–
H_3L	yes	yes	yes	yes	–	–	–	–
H_4L	yes	yes	yes	yes	–	–	–	–

[a]Prot. form stands for protonated form of a polyamine, The LEC stands for the lowest in electronic energy conformer, F-set = full set of LECs found after full optimization, R-set = reduced set of LECs as found from pre-optimization protocol. *(1) indicates that one new conformer was added to the set of LECs after full optimization.

Table S5. Step-wise selection of conformers needed and sufficient for protonation constants calculations using the 3-step (*EGB*), 4-step (*EEGB*) and most time-effective 5-step (*EEBGB*) protocol.* Data obtained for each tautomers are shown in PART (a) for 2,2,2-tet and PART (b) for 3,2,3-tet.

PART (a)			***EGB*-protocol**			***EEGB*-protocol**				***EEBGB*-protocol**				
2,2,2-tet + $4H_2O$	**MM confs**	**Step-1**	**Freq. calc.**	**Step-2**	**Step-3**	**Step-2**	**Freq. calc**	**Step-3**	**Step-4**	**Step-2**	**Step-3**	**Freq. calc**	**Step-4**	**Step-5**
L	30	7	7	4	3	6	6	4	3	6	3	3	3	3
HL_p	30	1	2	2	2	2	2	2	2	2	2	2	2	2
HL_s	30	1												
H_2L_{ps}	30	3	12	3	3	2	2	2	2	12	2	2	2	2
H_2L_{pp}	30	9												
H_3L	30	8	8	8	4	2	2	2	2	8	2	2	2	2
H_4L	30	5	5	3	3	3	3	2	2	4	2	2	2	2
Sum:	210	34	**34**	20	15	15	**15**	12	11	32	11	**11**	11	11

PART (b)			***EGB*-protocol**			***EEGB*-protocol**				***EEBGB*-protocol**				
3,2,3-tet $4H_2O$	**MM confs**	**Step-1**	**Freq. calc.**	**Step-2**	**Step-3**	**Step-2**	**Freq. calc.**	**Step-3**	**Step-4**	**Step-2**	**Step-3**	**Freq. calc.**	**Step-4**	**Step-5**
L	30	10	10	6	3	1	1	1	1	1	1	1	1	1
HL_p	30	8	21	6	4	3	3	2	2	3	2	2	2	2
HL_s	30	13												
H_2L_{ps}	30	11	13	3	2	1	1	1	1	3	1	1	1	1
H_2L_{pp}	30	2												
H_3L	30	12	12	5	5	3	3	2	2	3	3	3	2	2
H_4L	30	28	28	9	5	14	14	7	5	14	7	7	6	6
Sum:	210	84	**84**	29	19	22	**22**	13	11	24	14	**14**	12	12
Total:	420	118	**118**	49	34	37	**37**	25	22	56	25	**25**	23	23
%-total:		**28**	**28**	**12**	**8**	**9**	**9**	**6**	**5**	**13**	**6**	**6**	**5**	**5**

*MM confs = MM-generated conformers; **Step-1** is common to all protocol and it involves selection of lowest energy conformers (LECs) falling within 4 kcal/mol *E*-window from pre-optimization in Gaussian after 20 cycles; **Step-2** in ***EGB*-protocol** involves selection of LECs falling within 2 kcal/mol *G*-window after frequency calculation; **Step-3** in ***EGB*-protocol** involves selection of conformers with %-fraction > 5 after Boltzmann distribution on selected LECs in Step-2; **Step-2** in ***EEGB*-protocol** involves selection of LECs falling within 2 kcal/mol *E*-window after full optimization of conformers selected in Step-1; **Step-3** in ***EEGB*-protocol** involves selection of LECs falling within 2 kcal/mol *G*-window after frequency calculation; **Step-4** in ***EEGB*-protocol** involves selection of conformers with %-fraction > 5 after Boltzmann distribution on selected LECs in Step-3; **Step-2** in ***EEBGB*-protocol** is as Step-2 in *EEGB*-protocol; **Step-3** in ***EEEGB*-protocol** involves selection of conformers with %-fraction > 5 after Boltzmann distribution on selected LECs in Step-2; **Step-4** in ***EEEGB*-protocol** involves selection of LECs falling within 2 kcal/mol *G*-window after frequency calculation; **Step-5** in ***EEEGB*-protocol** involves selection of conformers with %-fraction > 5 after Boltzmann distribution on selected LECs in Step-4.

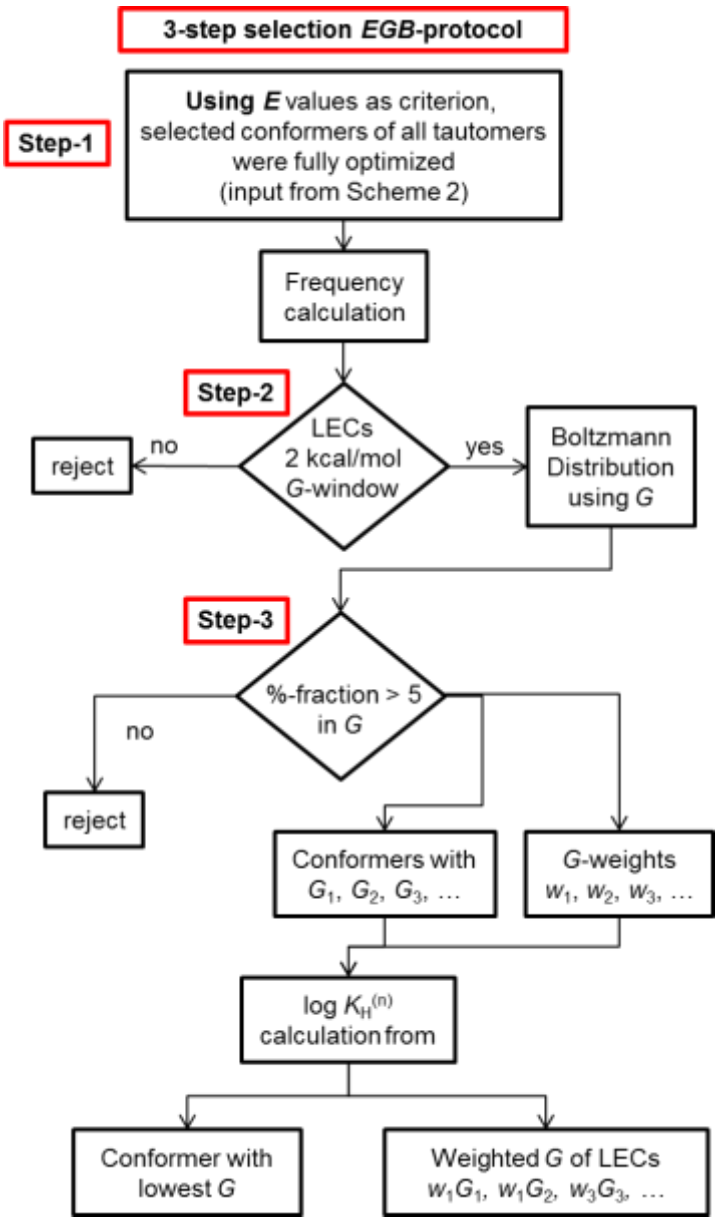

Scheme S2. Time most demanding and least accurate 3-step selection *EGB*-protocol tested for protonation constants calculations of polyamines.

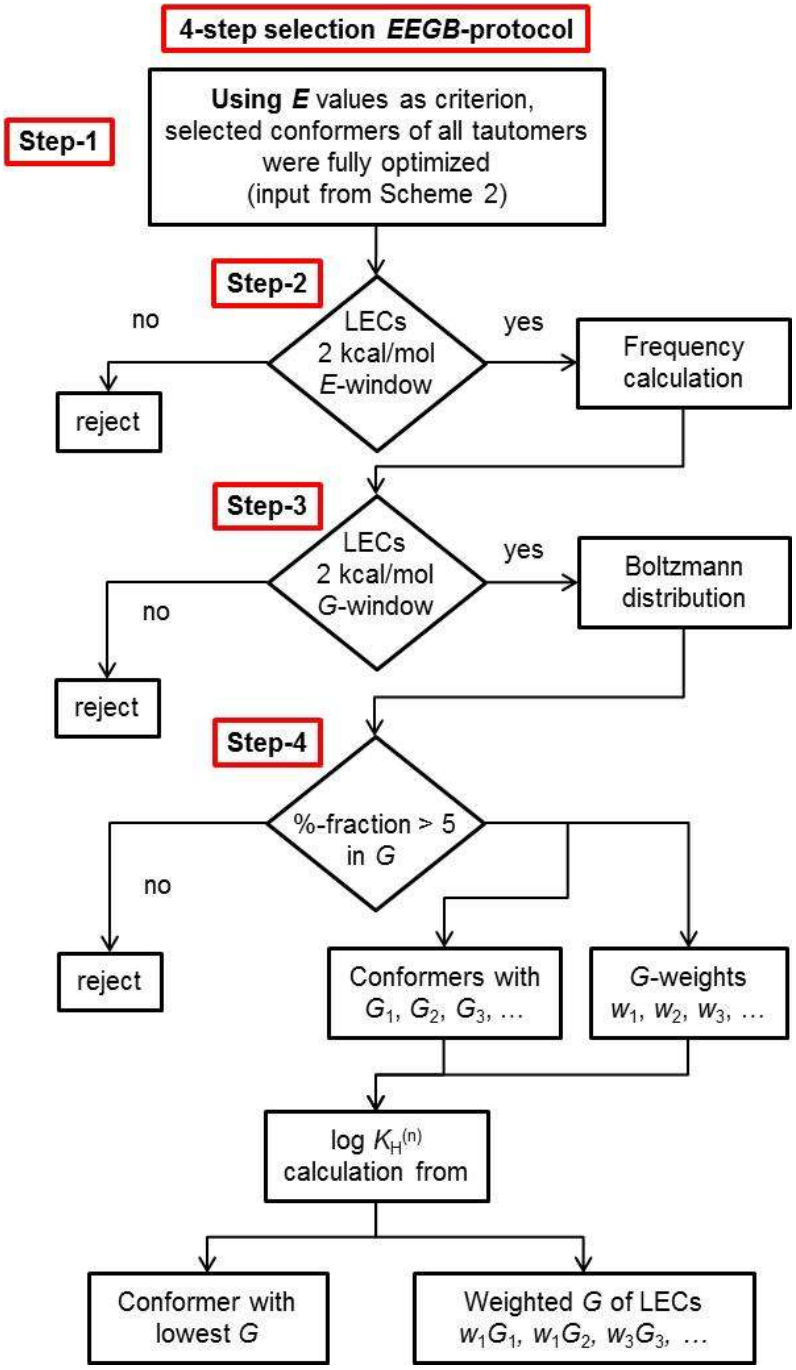

Scheme S3. Time efficient and well-performing 4-step selection *EEGB*-protocol tested for protonation constants calculations of polyamines.

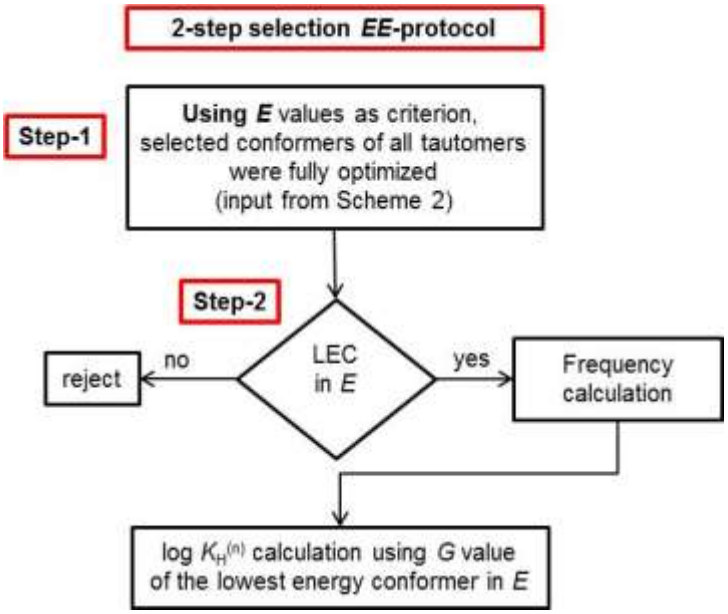

Scheme S4. 2-step selection *EE*-protocol tested for selection of conformers for protonation constants calculations.